AD-A189 068 STUDY OF PHOTOCHROMIC MATERIALS FOR USE IN OPTICAL SIGNAL PROCESSING(U) SAN DIEGO STATE UNIV CA DEPT OF PHYSICS J A DAVIS ET AL. NOV 87 RADC-TR-87-208 1/1

UNCLASSIFIED F/G 20/6 NL

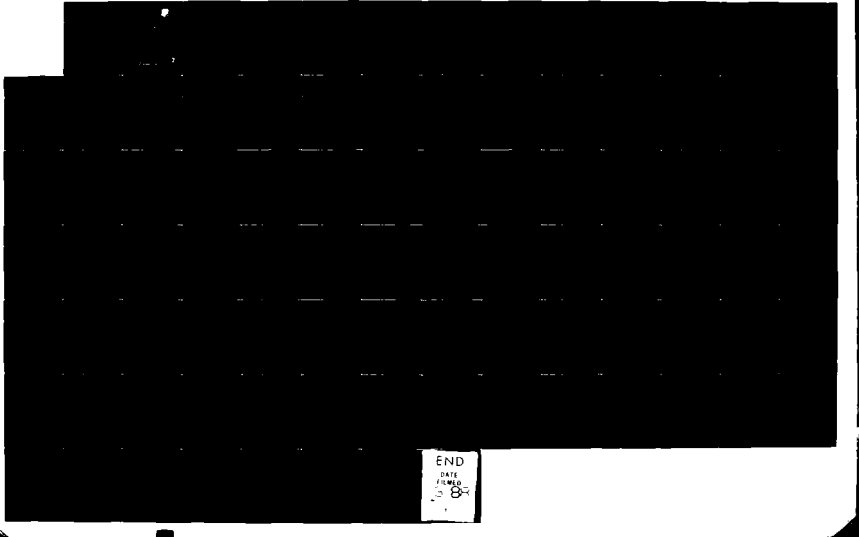

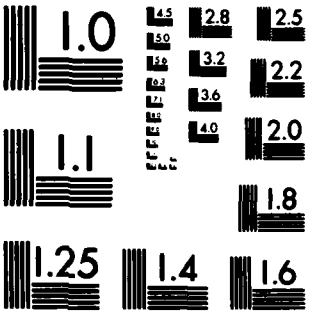

MICROCOPY RESOLUTION TEST CHART
NATIONAL BUREAU OF STANDARDS-1963-A

AD-A189 068

STUDY OF PHOTOREFRACTIVE MATERIALS FOR USE IN OPTICAL SIGNAL PROCESSING

[redacted]

[redacted]

UNCLASSIFIED
SECURITY CLASSIFICATION OF THIS PAGE

REPORT DOCUMENTATION PAGE

Form Approved OMB No. 0704-0188

1a. REPORT SECURITY CLASSIFICATION UNCLASSIFIED	1b. RESTRICTIVE MARKINGS N/A
2a. SECURITY CLASSIFICATION AUTHORITY N/A	3. DISTRIBUTION/AVAILABILITY OF REPORT Approved for public release; distribution unlimited.
2b. DECLASSIFICATION/DOWNGRADING SCHEDULE N/A	
4. PERFORMING ORGANIZATION REPORT NUMBER(S) N/A	5. MONITORING ORGANIZATION REPORT NUMBER(S) RADC-TR-87-206
6a. NAME OF PERFORMING ORGANIZATION San Diego State University 6b. OFFICE SYMBOL (If applicable)	7a. NAME OF MONITORING ORGANIZATION Rome Air Development Center (IRAP)
6c. ADDRESS (City, State, and ZIP Code) Department of Physics College of Sciences San Diego CA 92182	7b. ADDRESS (City, State, and ZIP Code) Griffiss AFB NY 13441-5700
8a. NAME OF FUNDING/SPONSORING ORGANIZATION Rome Air Development Center 8b. OFFICE SYMBOL (If applicable) IRAP	9. PROCUREMENT INSTRUMENT IDENTIFICATION NUMBER F30602-86-C-0085
8c. ADDRESS (City, State, and ZIP Code) Griffiss AFB NY 13441-5700	10. SOURCE OF FUNDING NUMBERS PROGRAM ELEMENT NO. 61011F; PROJECT NO. LDFP; TASK NO 07; WORK UNIT ACCESSION NO. C6

11. TITLE (Include Security Classification)
STUDY OF PHOTOCHROMIC MATERIALS FOR USE IN OPTICAL SIGNAL PROCESSING

12. PERSONAL AUTHOR(S)
Dr. Jeffrey A. Davis, Richard L. Lee

13a. TYPE OF REPORT	13b. TIME COVERED	14. DATE OF REPORT (Year, Month, Day)	15. PAGE COUNT
Final	FROM Jun 86 TO Jun 87	November 1987	92

16. SUPPLEMENTARY NOTATION
This effort was funded totally by the Laboratory Directors' Fund

17. COSATI CODES			18. SUBJECT TERMS (Continue on reverse if necessary and identify by block number)
FIELD	GROUP	SUB-GROUP	Photochromics, Spatial Light Modulators, Optical Storage, Optical Filters
14	03		
20	03		

19. ABSTRACT (Continue on reverse if necessary and identify by block number)
This report summarizes 12 months of investigation into the feasibility of using photochromic materials for programmable spatial filters and optical data storage applications. Write and erase times, optical density, and laser power intensity measurements were made.

(Keywords: ———)

20. DISTRIBUTION/AVAILABILITY OF ABSTRACT	21. ABSTRACT SECURITY CLASSIFICATION
☒ UNCLASSIFIED/UNLIMITED ☐ SAME AS RPT ☐ DTIC USERS	UNCLASSIFIED
22a. NAME OF RESPONSIBLE INDIVIDUAL Kevin W. Devaney, Capt, USAF	22b. TELEPHONE (Include Area Code) (315) 330-4581
	22c. OFFICE SYMBOL RADC (IRAP)

DD Form 1473, JUN 86 Previous editions are obsolete. SECURITY CLASSIFICATION OF THIS PAGE
UNCLASSIFIED

Table of Contents

Chapter I - Introduction

The purpose of this report is to characterize photochromic samples containing mercury dithizonate for possible use in optical signal processing applications. Before discussing photochromism, we briefly review the optical signal processing applications under consideration.

One of the most successful applications of optical signal processing is in an rf spectrum analyzer as shown in Fig. 1. An input rf signal consisting of a number of frequency components having different amplitudes is used to drive a Bragg cell AOLM.

The AOLM uses a transducer driven by the rf signal to generate a sound wave within a solid block (often of glass). The compressions and rarefactions of the sound wave cause the density of the glass to vary periodically acting as a phase diffraction grating.

The spacings of this phase grating depend on the particular frequency components of the rf signal while the amplitudes of these components determine the depth of the phase grating.

A laser beam incident on the glass block will therefore undergo diffraction by this grating. If the rf signal has a series of spectral components, the incident laser beam will be diffracted into different angles simultaneously. The intensities and angles of the diffracted light correspond to the intensity and frequency of each Fourier component in the rf spectrum.

Therefore, the diffraction pattern from the AOLM represents the Fourier transform of the rf spectrum. This can be realized in the near field limit at the back focal plane of a lens. Hence, the Fourier spectrum of the rf signal is found at the back focal plane of an optical lens.

The Fourier spectrum can be analyzed by placing a photodiode array in this back focal plane. Each diode will record a small frequency interval. The intensities of the Fourier components of the rf spectrum can then be read out. This example illustrates the parallel advantages of optical signal processing. The entire Fourier spectrum is being analyzed at the same time.

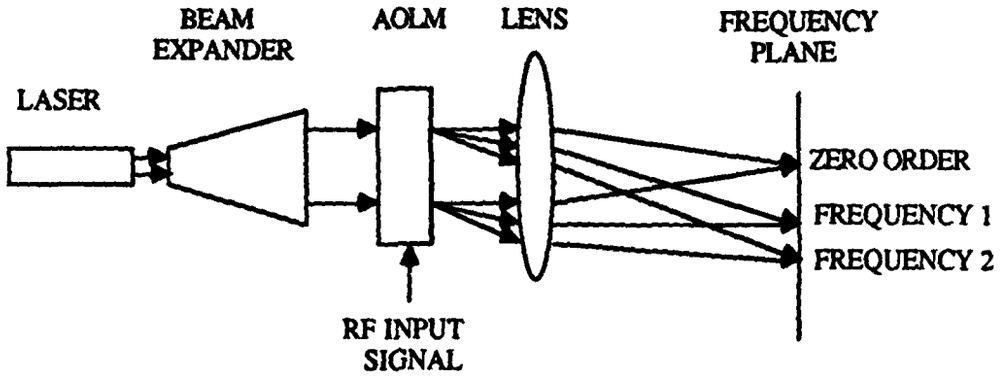

Fig. 1 Schematic Outline of RF Spectrum Analyzer

However, the existence of a huge rf component at one frequency (called a jamming signal) can saturate a number of elements in the photodiode array limiting the resolution of the device. If an opaque mask is placed at that physical location corresponding to the jamming frequency, the huge optical signal will be prevented from reaching the photodiode array (or excised). Of course, if the rf jamming signal frequency were to be altered, then the location of the opaque mask would have to be changed.

One candidate for a programmable opaque mask consists of a photochromic material whose optical absorption for a certain wavelength may be increased by illuminating a desired sample location with light of another wavelength. It is the purpose of this study to evaluate these photochromic samples for their potential in this application. Mercury dithizonate was chosen since its writing and reading wavelengths

correspond with commercially available laser wavelengths. A thorough review of photochormism is presented next.

Photochromism is the reversible, photo-induced change in the absorption spectrum of a material upon optical illumination. As discussed above, the photo-induced absorbance change in the photochromic material may be used as a basis to perform optical data storage and optical signal processing. Unlike material ablation techniques used in today's optical data storage systems which offer only "write-once, read-only" media , photochromic materials offer the user the advantages of a reusable material. Photochromic materials can be relatively inexpensive and offer high resolution data storage and real time signal processing applications. It was the general goal of this work to characterize two types of photochromic molecules (encased in a plastic polymer) for their ability to change their absorption spectra under certain experimental conditions. In order to better understand the photochromic process, the following provides an introduction to photochromism.

Ground state photochromic molecules characteristically absorb within an ultraviolet or visible wavelength band. Upon absorption of this energy, the molecules undergo a reversible rearrangement, resulting in excited state molecules. The excited state absorbs predominately in a longer wavelength region than that of the ground state. The absorbance of the original band diminishes as the number of excited photochromic molecules increases. Hence, as the forward excitation reaction proceeds, one observes a decrease in the ground state absorption band and an increase in the excited state absorption band. Once the excitation, or write, light is removed from the sample, the excited molecules revert back to the ground state leading to an increase in the ground state absorption peak with a decrease in the excited state absorption peak. A unique absorption spectrum is associated with each of the two states and the excitation and relaxation reactions may be followed by monitoring changes in the absorption spectrum at λ_2, .

One may functionally represent the reversible photochromic process as

$$A(\lambda_1) + hc/\lambda_1 \text{ ——— } A^*(\lambda_2) \quad \text{(excita ion)}$$

$$A^*(\lambda_2) \text{ ——— } A(\lambda_1) \quad \text{(relaxation),}$$

where $A(\lambda_1)$ represents the ground state molecule which absorbs at λ_1 and $A^*(\lambda_2)$ represents the excited state molecule which absorbs at λ_2. The absorption of the incident optical energy by the ground state molecule causes the molecule to isomerize to an excited state and hence the activation reaction is strongly dependent on the intensity of the excitation radiation. The excited state represents a different molecular configuration from that of the ground state. During the relaxation of the excited state, the molecule rearranges itself to the ground state configuration. Since the relaxation reaction requires the rearrangement of part of the molecule in the absence of optical radiation, the back reaction is highly temperature dependent. The relaxation to the ground state may occur over a relatively long time period if the temperature is low.

The light-induced changes in the absorption of a photochromic species may be followed spectroscopically as a function of time. Two general changes in the absorbance spectra of photochromic molecules are observed when they are illuminated with visible light. First, there is a decrease in the absorbance at the ground state absorbing wavelength band. Concurrently, there is an increase in the absorbance of the photochromic material at a wavelength longer than that of the original band. As the exposure of the sample to the activating light increases, the ground state absorbance continues to decrease while the excited state absorbance increases.

There are many different chemical species which display photochromism, such as benzospirans (1), stibenes (1), and some polymers (2). Many of these species are used in sunglasses, trace metal analysis, and optical displays (1). There are two drawbacks to these systems. First, most of the materials used in these cases are sensitive to the ultraviolet wavelength region. Sources and optical elements for use in this wavelength region are often difficult to obtain. Secondly, the amount of ultraviolet energy available

from the usual high intensity sources is limited. Thus, past studies of photochromism have often been hampered due to the mismatch between available sources and materials.

An alternate system which responds in the visible spectrum involves the molecular species diphenylthiocarbazone, or dithizone, whose photochromic behavior has been investigated in solutions of carbon tetrachloride and chloroform (3) and hexane (4). If a metal atom is attached to the dithizone structure, its photochromic properties are enhanced(3). Examples of those metals which form a complex with dithizone include platinum, palladium, silver, and mercury. Of these compounds, the mercury dithizonate species shows the slowest return to the ground state from the excited state (3). The mercury dithizonate species also shows high conversion efficiency from the ground state to the excited state. All of these metal complexes show major ground state absorption peaks in the blue-green wavelength region (3). Two of the mercury dithizonate compounds, mercury bisdithizonate and phenyl mercury dithizonate, have absorption peaks of the ground and excited states in the 480 - 510 nm. and 600 nm. regions, respectively (3). These are important characteristics, since high quality optical elements are readily available for use in the visible wavelength region. More importantly, lasers capable of delivering high input energy in these wavelength regions are commercially available. These characteristics make the mercury dithizonate species particularly suitable as inexpensive, reversible media for high speed optical information storage and optical data processing.

It was the purpose of this work to characterize the writing and relaxation times associated with these two types of photochromic mercury dithizonate molecules bound in a cellulose acetate butyrate (CAB) plastic film. Each of the molecular species were examined for its ability to change states when exposed to light of wavelength 488.0 nm. or 514.5 nm. The time dependence of both the excitation and relaxation reactions were followed and their reaction times determined. The dependence of the reaction times on such factors as temperature, incident write light intensity, write light wavelength,

species type, and species concentration is presented. The following outlines the general flow of the remainder of the report.

Chapter II introduces the theoretical aspects of the photochromic process. The excitation and relaxation reactions are discussed. The reaction kinetics of the relaxation reaction are examined and the dependence of the reaction times on several experimental parameters is discussed. Chapter III describes the experimental setups used to perform the experiments. Each major piece of equipment is discussed in detail in order that its role in the overall system may be understood for future studies if needed. Limitations of some of the equipment and methods which were used to improve performance are included. Chapter IV presents some UV-visible spectral data of the plastic samples used in this study in order to better understand the photochromic behavior associated with each sample. Chapter V discusses the general experimental observations regarding the laser-induced changes in a photochromic system at different temperatures. Chapter VI discusses the results of temperature-dependent relaxation reactions associated with the return of the excited state photochromic molecules to their ground state configuration. Reaction constants and decay times of the relaxation reaction are presented and discussed. Chapter VII discusses the wavelength dependence of the excitation reaction. Experimental excitation, or writing, data obtained using both the 488.0 nm. and the 514.5 nm. wavelength lines of an argon ion laser are presented. The dependence of the excitation reaction on the photochromic sample composition is also discussed. Chapter VIII provides the results of some high speed writing experiments designed to see how fast one may write onto the photochromic samples. And finally, Chapter IX provides a brief discussion of the conclusions reached as various experimental parameters were varied.

This report is based upon the M.S. thesis written by Richard Lee and modified for this report by Dr. Jeffrey Davis.

Chapter II - Theory

The absorption of activating light by ground state photochromic molecules causes a tautomerism, or a shift in the equilibrium between two different states, or isomers. The shift in the equilibrium concentrations of the two isomers leads to a shift in the major absorption peaks of the system. This tautomeric description is the most general one responsible for photochromism.

On the molecular level, photochromism represents a change in the extended electronic structure responsible for the absorption of light in the ultra-violet and visible regions. A change in the electronic structure of a molecule results in a new absorption band. The ground state electronic structure of photochromic molecules allows them to absorb predominantly in the ultraviolet to blue-green wavelength region. Absorption of light in this region causes an excited state to occur which absorbs at a longer wavelength. A specific example of this is the heterolytic photoisomerization of spiropyrans (1). The activating light specifically causes a heterolytic cleavage of part of the molecule. This newly formed species absorbs light of a different spectral band. Another example of a reversible, tautomeric change observed in organic solutions containing certain photochromic molecules is a photo-induced proton transfer between the surrounding medium and the photochromic molecule. This proton transfer leads to the formation of an isomer having a new absorption spectrum. Proton transfer accounts for the photochromic activity of 2-naphthylamine (1). A third mechanism of photochromism is trans-cis isomerization. In this mechanism, absorption of the excitation light causes a part of the ground state molecule to flip about a double bond, resulting in a new extended electronic structure. This is the mechanism involved in the excitation of photochromic mercury dithizonate (1). The cis-excited state is less stable

than the trans-ground state molecule and thermal relaxation will readily occur. Since the excited state is energetically unstable, the relaxation of the molecule to its more energetically favorable ground state may be expected to be temperature dependent. Each of these mechanisms usually represents single-step reactions, but more complicated systems can involve some combination of them as well as others not described here.

In this study, two photochromic species which are bound in a plastic matrix are examined. One species is mercury (II) bisdithizonate. The ground state configuration of mercury bisdithizonate is shown in Figure 2. Absorption by the molecule of the excitation light causes the ground state molecule to isomerize to the excited state configuration. Both of the two ligands of the molecule follow the same isomerization mechanism. However, the two ligands of the mercury bisdithizonate compound are presumed to isomerize independently of one another (5).

One mechanism for the isomerism from the ground state to the excited state includes the breaking of the hydrogen bond between the hydrogen on N_4 and the sulfur atom with the subsequent release of the hydrogen from the nitrogen atom. This leads to the formation of a double bond between N_3 and N_4 and a single bond is formed between N_3 and the carbon atom. The N=N-Phenyl group is now able to rotate about the newly formed C-N_3 single bond. A double bond is also formed between the sulfur atom and the carbon atom and the Hg-S covalent bond is changed to a coordination bond. The formation of the coordination bond between the sulfur atom and the mercury atom leads to the covalent bonding of N_1 and the mercury atom. The N_1-Hg bond further leads to the formation of a single bond between N_1 and N_2. The N_2 atom now accepts a hydrogen proton which is able to stabilize the rotation of the molecule by forming a hydrogen bond with N_4. The resulting molecular configuration represents the excited state of the mercury dithizonate molecule and is shown in Figure 3. This isomer is less stable than the ground state isomer and may revert back to the ground state spontaneously.

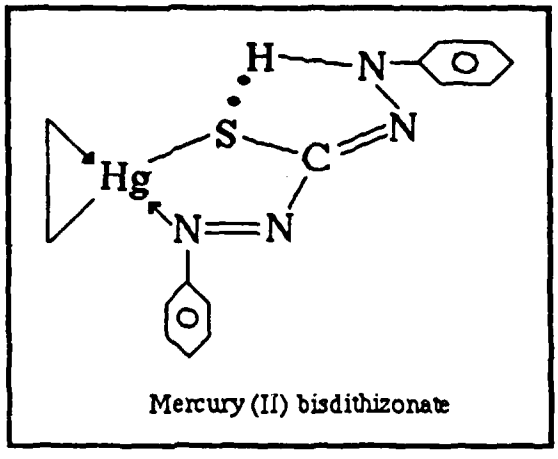

Figure 2. Structure of ground state mercury (II) bisdithizonate.

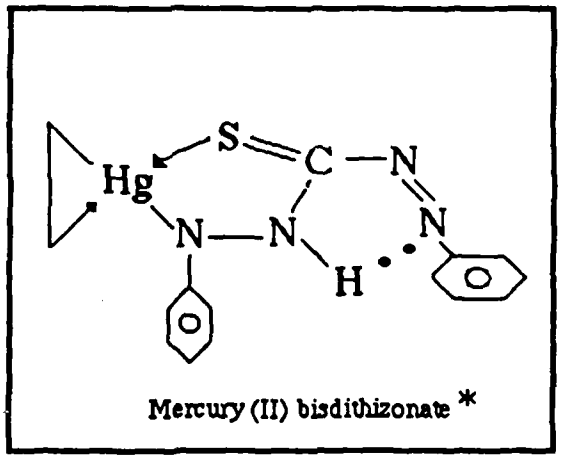

Figure 3. Structure of excited state mercury (II) bisdithizonate.

The other species used in this study is phenyl mercury dithizonate. The ground state and excited state molecules of phenyl mercury dithizonate are shown in Figures 4 and 5, respectively. The mechanism of excitation is the same as that of the mercury bisdithizonate, but in this case, only a single ligand per molecule is involved.

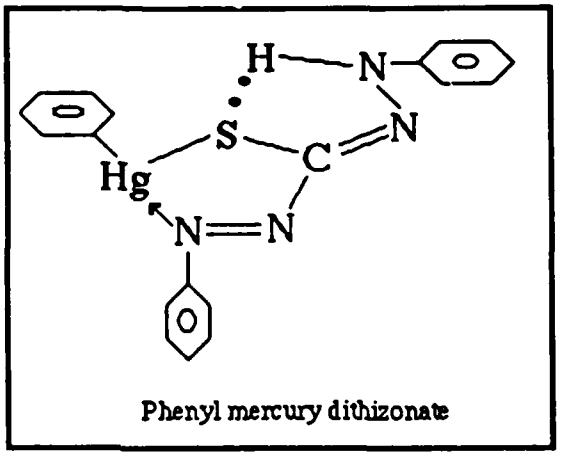

Figure 4. Structure of ground state phenyl mercury dithizonate.

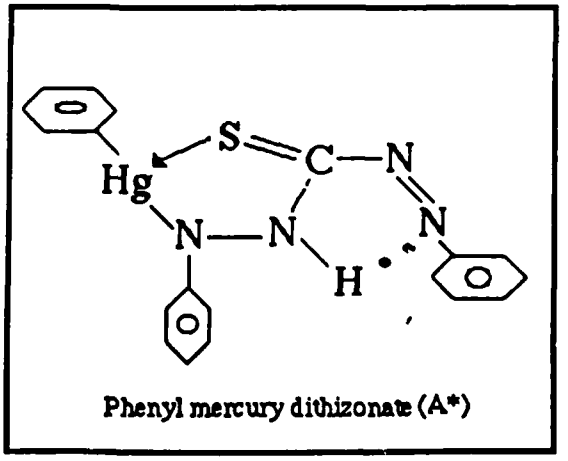

Figure 5. Structure of excited state phenyl mercury dithizonate.

Photochromic excitation and relaxation

The forward excitation reaction requires optical excitation of the photochromic molecules from the ground state to an excited state. The rate of the forward excitation reaction increases as the temperature increases since the rise in the kinetic energy of the molecules helps in the isomerism of the molecule. Once in this excited state, the molecule is energetically unstable and may relax back to the ground state. The primary mechanism for the relaxation, or decay, of the excited state to the ground state is the thermally induced isomerism of the excited state. The relaxation isomerism takes place independently of the excitation light. The dependence of the excitation and relaxation reactions on temperature and photochromic concentration will be discussed in the next sections.

Figures 6, 7 and 8 illustrate the photochromic excitation and relaxation processes for several tautomeric mechanisms using potential energy diagrams. Figure 6 shows the small energy barrier between the ground and excited states associated with thermochromic tautomers. Since the energy required to change states is small, these isomers may readily interconvert with changes in temperature. This mechanism also allows for the excitation of the ground state molecule via optical absorption and so is also photochromic in nature. Figure 7 shows a large forward reaction energy barrier. The large energy barrier indicates that conversion from the ground state to the excited state requires more energy than is available solely from thermal means. Thus, optical excitation is needed for this forward reaction. However, relaxation from the excited state to the ground state may take place thermally, since the energy required to go in this direction is small. The photochromic behavior of the mercury dithizonate molecules used in this study most closely follows this pattern. The mercury dithizonate is activated to its excited state by blue-green light and may thermally relax without the input of additional optical energy.

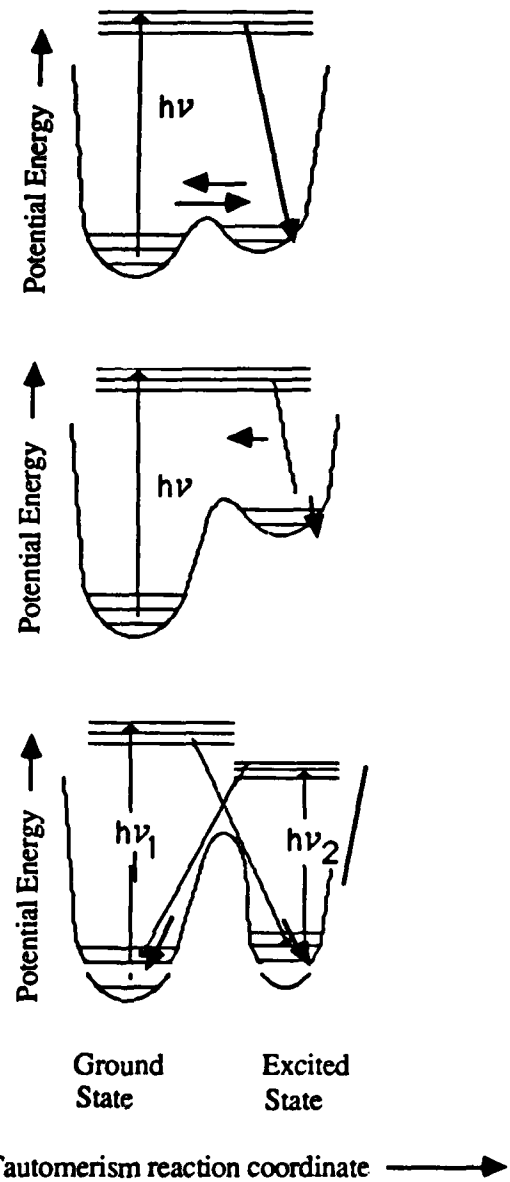

Figures 6, 7, 8. Potential energy diagrams for three different photochromic tautomeric mechanisms. Figure 6: normal tautomerism with equilibrium shifted photochemically and thermochemically; Figure 7: photochemical tautomerism with spontaneous reversion possible; Figure 8: photochemical tautomerism with light-induced reversion.

However, it is observed that, if the photochromic mercury dithizonate sample is strongly illuminated with red light, which is highly absorbed by the excited molecules, then an increase in the relaxation rate of the excited molecules occurs. This behavior is also observed in cases of strict photochromism. Figure 8 illustrates an extreme case of this strict photochromic behavior. The energy barrier is so high that optical energy is required for both the excitation and relaxation reactions and the mechanism is essentially thermally independent. Once the molecule is in a particular state, it will stay in that state until switched to the other state with the input of optical energy. As noted previously, the photochromism of the mercury dithizonate species most closely follows diagram in Figure 7, but also shows evidence of the enhanced optical relaxation as seen in Figure 8. However, the relaxation enhancement due to the read beam is small if the read beam intensity is kept low, as was the case in this study. Studies of the photo-induced relaxation reaction of CAB samples containing mercury bisdithizonate and mercury phenyl dithizonate are currently being done at San Diego State University by Tony Halloway (6). Previous studies of the photo-induced relaxation reaction of CAB samples containing a possible mixture of mercury bisdithizonate and mercury phenyl dithizonate have been done at S.D.S.U. by Mary Thomas (7).

The excitation and relaxation reactions of the mercury dithizonate samples may also be affected by impurities or other absorbing components in the photochrome-plastic system. In this case, since the chemical reactions used to produce the mercury dithizonate-polymer system rarely yield 100% of the desired product, remnants of the original reacting species, dithizone, may be present in small amounts in the final photochrome-polymer system. Since dithizone is modestly photochromic (4), care should be taken in the interpretation of results obtained from experiments which monitor the transmission of the photochromic reaction as a function of time.

A general discussion of the photochromic excitation reaction will be given next in terms of optical energy input and the time required to reach a particular optical density of

the material. After the optical excitation reaction is presented, the relaxation reaction is discussed in terms of its general dependence on the excited state photochrome concentration and, more specifically, on its thermal dependence. Since the observations associated with the relaxation of the mercury bisdithizonate and phenyl mercury dithizonate may be affected by the presence of other photochromic species (notably dithizone) within the polymer, a theoretical look at how the relaxation reaction rate is affected when more than one absorbing species is present will also be discussed.

Optical excitation of the ground state photochromic molecules

Consider a material of thickness d containing a random distribution of photochromic molecules. The material may be broken up into many thin slabs of thickness Δd. The photochromic molecules have some wavelength-dependent absorbance, $\epsilon(\lambda_1)$ per unit concentration C. A uniform and continuous beam of light of the excitation wavelength λ_1, and intensity I_0, is incident onto the face of the material. A read beam of low intensity and wavelength λ_2 is also incident onto the material. The molecules within the first slab will absorb some of the excitation radiation and become excited. Those in the next thin slab will absorb their share of the attenuated throughput from the first slab. Each successive slab will likewise absorb the attenuated activating optical radiation. Any light which is not absorbed will be transmitted through the sample. The molecules in each thin slab which absorbed the excitation radiation are now in their excited state and their absorption peak has shifted to the red wavelength region. The absorbance at the λ_2 wavelength increases with an increase in the number of excited molecules. As the exposure time increases, the number of molecules which become excited increases until an equilibrium level is reached in which the forward and back reactions approach a steady-state condition. At this point, no further decrease in the transmission of the monitoring read beam will be observed as long as the excitation beam is incident on the sample.

In order to excite a given number of photochromic molecules, a certain amount of optical energy is required. Each species of molecule has an absorption coefficient associated with it which is dependent on wavelength. Ordinarily, the conversion efficiency to the excited state increases as the absorption coefficient for a specific wavelength increases. As the input energy is increased, the number of ground state to excited state transitions also increases. For photo-sensitive media such as photographic film, a plot of the optical density vs. the logarithm of the exposure energy yields a characteristic HD curve as illustrated in Figure 9 (8). At low exposure energies, the curve is relatively flat along a minimum optical density. As the exposure energy increases, the optical density begins to increase linearly with the logarithm of the energy. This behavior measures the excitation of the photosensitive molecules as the energy is increased. Once the exposure energy reaches a particular level, the optical density no longer changes appreciably, but saturates. Further input of optical energy does not change the number of excited state molecules. The photochromic samples used in this study presumably follow this same general behavior as the photographic film.

The exposure energy required to reach any desired optical density along the characteristic curve is dependent on the product of the exposure time and exposure intensity, and is normally not singularly dependent on either the time or the intensity. This relationship between the exposure time and the exposure intensity is summed up in the Reciprocity Law:

$$I \times t = K, \tag{1}$$

where the intensity I, is given in Joules per second per unit area, and the time, t, is measured in seconds. K represents a specific exposure which would lead to a particular optical density of the material, and has units of energy per unit area. This relationship may be rewritten as

$$\ln I = -\ln t + \ln K. \tag{2}$$

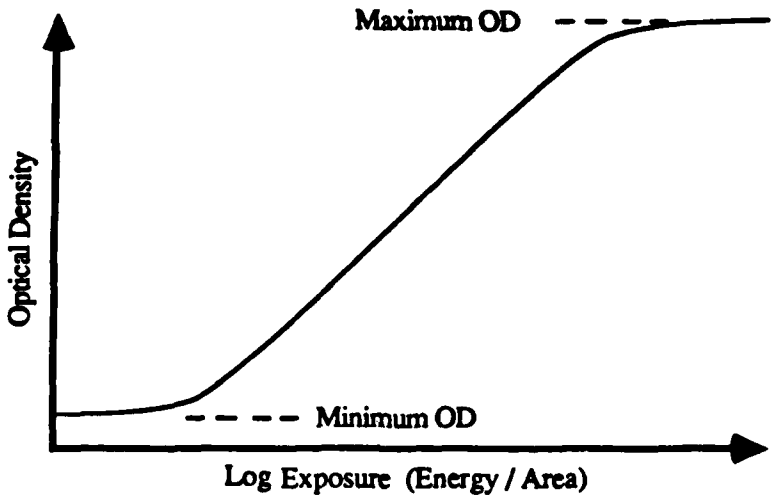

Figure 9. Typical characteristic HD curve for photosensitive materials.

A plot of the natural logarithm of the intensity vs. the logarithm of the time required to reach a specified optical density (at a specified temperature), should yield a straight line with unit slope. By varying the intensity of the activating beam of light and measuring the time required to reach a particular optical density, one may experimentally verify this relationship. It is to be noted the Reciprocity Law may not be followed at very low or very high incident intensities. A low exposure intensity may lead to an extraordinarily long exposure time to reach a particular optical density, since the equilibrium population of excited molecules is relatively small due to the depletion of the excited state population by the relaxation reaction. On the other hand, a high exposure intensity will result in the rapid excitation of of photochromic molecules within the first thin layer of the sample. This rapid increase in the excited state population within a small sample depth will attenuate the read beam intensity and may not fully represent the photochromic process throughout the entire depth of the plastic.

The optical sensitivity of the material increases as the number of absorbing molecules in the material increases. In order to follow the changes in a photochromic sample's optical sensitivity as the number of excited state molecules changes, one must

look at some of the relationships which relate the concentration of absorbing molecules to the optical density of the material. The next section discusses these relationships through the use of Beer's Law.

Beer's Law

The transmission of optical radiation through a material can be related to the concentration of the absorbing species through Beer's Law (9). For a thin sample of material of thickness d, the transmittance of light through the material is given by

$$\log (I_0/I) = \epsilon(\lambda)C(t)d , \qquad (3)$$

where C(t) is the time-dependent concentration of absorbing species in moles per liter, $\epsilon(\lambda)$ is the molar absorptivity of the species (associated with the incident wavelength) in liters per mole per centimeter, I is the transmitted intensity, and I_0 is the incident intensity. Both I and I_0 have units of watts per cm^2. Beer's law works best for dilute and homogeneous concentrations of absorbing materials and deviations from this simple relation may occur if the samples contain too much absorbing material.

The optical density (OD) of a transmitting medium is defined as

$$OD = - \log (I/I_0) . \qquad (4)$$

If the concentration of absorbing species changes with time, then the optical density will also change with time. Equations (3) and (4) may be combined to yield

$$OD(t) = \epsilon(\lambda)C(t)d . \qquad (5)$$

By monitoring the optical density during the course of the reaction, one may follow the changes in the concentration of a specific absorbing species.

Figure 10 shows the general experimentally observed behavior of the activation and relaxation cycle of a photochromic system when λ_2 is monitored. T_A represents the time the excitation, or write, beam is turned on. The transmitted HeNe intensity begins to decrease immediately due to the increase in the number of excited state molecules. The transmitted HeNe intensity eventually reaches an equilibrium saturation level. The saturation level represents the final tautomeric equilibrium due to the interconversion of

the photochromic isomers for a given temperature and incident write beam intensity. The equilibrium between the two isomers illustrates a competition which is occurring between the ground state and activated states of the photochromic molecules. The incident write beam is promoting ground state molecules into the excited state while, concurrently, thermal relaxation of the excited molecules is occurring. An increase in the incident write beam intensity shifts the equilibrium toward the excited state, while an increase in temperature shifts the equilibrium toward the ground state molecular configuration. The saturation depth of the optical density of the read beam will therefore depend on the sample temperature and the relative numbers of excited and ground state molecules at equilibrium. The saturation optical density will generally increase with an increase in the incident write beam intensity for a given temperature. Likewise, the saturation optical density will generally decrease with an increase in temperature for a given (moderate) intensity of the incident write beam.

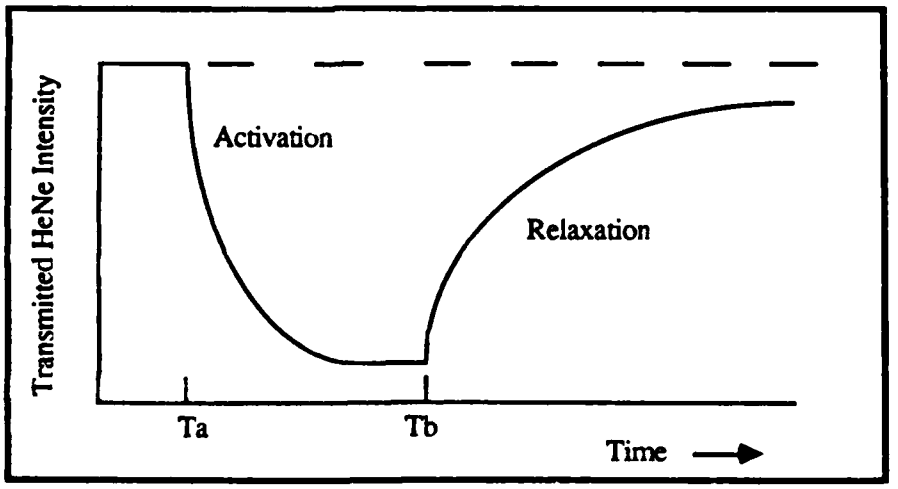

Figure 10. General behavior of the transmitted HeNe probe beam intensity as a function of time for the excitation-relaxation cycle of a photochromic material. T_A represents the time when the write beam is turned on. T_B represents the time when the write beam is turned off.

If the write beam is now removed from the system at time T_B, the transmitted HeNe intensity begins to increase. The excited molecules are thermally relaxing back to the ground state, hence the absorption of the monitoring read beam decreases. The transmission of the read beam will continually increase and eventually reach its original value.

The overall excitation and relaxation behavior of the photochromic molecules has been presented and discussed. Since the relaxation of the excited photochromic molecules is thermally dependent and does not require any incident optical energy, the relaxation process may be examined in detail as a temperature-dependent reaction. The following section discusses a mathematical approach of analyzing the relaxation of a photochromic system.

Thermal relaxation

Thermal relaxation of the excited molecules continually occurs throughout the photochromic process. Even when the excitation light is incident onto the photochromic sample promoting the molecules into their excited state, relaxation of the molecules takes place. However, due to the presence of the incident excitation light, the equilibrium is shifted in favor of the excited state. This is due to the tautomerism which is exhibited by the relative concentrations of the two species. The tautomeric shift in the equilibruim concentrations of the two isomers is induced by the excitation light. Once this excitation light is removed, the excited molecules thermally relax back to their ground state configuration. A relatively high temperature will cause an increase in the cis-trans isomerization of the excited molecules to the ground state. Conversely, a low temperature will slow the rate at which the excited molecules relax back to their ground state.

Temperature will also affect the plastic matrix surrounding the photochromic molecules. A high temperature will allow the individual polymer strands of the matrix to have a larger average interchain spacing and allow for an easier physical transition of the excited molecules to their ground state configuration. A low temperature will reduce the motional freedom of the plastic matrix, thereby reducing the rate of the reverse rearrangement of the excited state molecules.

If the return reaction involves only a single type of excited molecule and follows a relaxation mechanism which is independent of all neighboring molecules, then one may describe the back reaction via the first-order rate law

$$- d[A^*] /dt = k[A^*] . \quad (6)$$

Equivalently, one may write

$$[A^*]_t = [A^*]_0 \exp(-kt) , \quad (7)$$

where $[A^*]_0$ refers to some initial (high) concentration of excited molecules, $[A^*]_t$ refers to the concentration of excited molecules some time t after the excitation light has been removed and k represents the reaction rate constant. The reciprocal of the rate constant represents the time, tau (τ), required to reduce the number of excited state molecules to 1/e of their original value. The rate constant is temperature dependent since we are dealing with the isomerism between a less energetically favorable state and a more favorable one. Thus, an increase in the sample temperature will lead to a faster relaxation rate.

The optical density is proportional to the concentration of light-absorbing species according to Equation (5). Since first order kinetics are assumed, then combining Equations (5) and (7) reveals a linear relationship between the natural logarithm of the optical density and the reaction time:

$$\ln OD_t = -kt + \ln OD_0 . \quad (8)$$

An experimental plot of the natural log of the optical density vs. time should yield a linear relationship with a slope of -k.

The rate constant k for the first order relaxation reaction, is a measure of the ability of the excited state molecule to relax back to the ground state configuration. The number of molecules which have sufficient energy to overcome the thermodynamic reaction barrier in Figure 6 (middle figure) and revert to the ground state configuration is a function of temperature and the rate of the relaxation reaction follows a Boltzmann distribution. The rate constant, k, may be described by the Arrhenius equation (10),

$$k = P \exp(-E_a / k_b T) . \qquad (9)$$

In this expression, E_a represents the activation energy of the reaction, k_b is Boltzmann's constant, and T is the temperature in degrees Kelvin. The term P is a preexponential factor which represents a kind of fundamental frequency comparable in magnitude to molecular vibrations and has units of sec^{-1} (10). Equation (9) may be written in a more practical fashion as

$$\ln k - \ln P = -E_a / k_b T \qquad (10)$$

or

$$\ln (1/k) = (E_a / k_b T) - \ln P , \qquad (11)$$

where 1/k represents the relaxation time, τ, of the reaction. By experimentally determining k at several temperatures, one may plot $\ln \tau$ vs. inverse sample temperature and estimate the energy of activation for the relaxation process from the slope of the line, if the proposed model of the photochromic process is correct.

If more than one species of excited molecules (with common absorption profiles) are independently relaxing to the ground state via first order kinetics, then one will have separate rate constants, k_1, k_2, k_3, etc. which govern the relaxation rate for each species. These various rate constants will result in a nonlinear Arrhenius plot of $\ln \tau$ vs. inverse temperature. The fastest rate constant will dominate in the very early stages of the relaxation while the intermediate rates will tend to dominate in the middle of the overall reaction and only the slowest rate constant will be evident as the reaction time

increases. The samples used in this study presumably contain a single species of photochromic molecules, and first order kinetics appear sufficient to explain our data.

Chapters IV through VIII will use the ideas and equations developed in this chapter to analyze data obtained from experiments designed to monitor the photochromic excitation and relaxation processes. Before the results of the experimental observations of the photochromic excitation and relaxation reactions are presented, a detailed look at the experimental setups and methods used to examine these photochromic processes in plastic samples containing mercury bisdithizonate and phenyl mercury dithizonate will be given in the following chapter.

Chapter III - Experimental Techniques

The main objective of this work was to characterize the photochromic excitation and relaxation reactions which occur when plastic samples containing either mercury bisdithizonate or phenyl mercury dithizonate molecules are exposed to an excitation light beam. This characterization was done by monitoring the changes in the absorption of the samples at the photochrome's excited state absorption wavelength as the number of excited state photochromic molecules was increased by an incident light beam of wavelength λ_1. Experimentally, the transmittance of a HeNe read beam of wavelength 632.8 nm. (which is near, but not at, λ_{2max} of the photochromic molecules) was monitored as a function of time through plastic samples containing light-absorbing photochromic molecules during and after exposure to an argon laser beam of wavelength 488.0 nm. or 514.5 nm. The characterization of the samples was done under various experimental conditions of sample composition and temperature as well as different activating light intensities.

This chapter provides a discussion of the methods and components which were used to vary the conditions imposed on the photochromic samples during the characterization experiments. Experimental setups used to characterize the photochromic samples were divided into three intensity-dependent configurations. Each of these different setups provided a different range of write beam intensities. The three intensity ranges used in this study were 10 - 50 mW/cm^2, 10 -150 W/cm^2, and 200 - 800 W/cm^2. Some of the methods and components which were used were common to each of the different experimental setups, while other components or methods were unique to a particular setup. The next section provides an overview of those techniques which were common to all of the experiments. A detailed discussion of the components and

techniques is included while presenting the low intensity experimental setup. The final sections of this chapter discuss the procedures and components which were unique to the medium and high intensity experimental setups.

Experimental techniques common to all setups

Figure 11 shows the typical experimental setup used throughout the characterization experiments. The sample was illuminated with light from a Coherent model 90-3 argon laser using either the 514.5 nm or the 488.0 nm wavelength. This laser provides a maximum output power of 1 W using the 488.0 nm. line or 1.4 W using the 514.5 nm. line. Various lens configurations were used to vary the spot size of the argon laser beam and the size of the writing intensity. In addition, the sample was also illuminated with light from a Uniphase model 1103P helium neon laser with an output power of 2 mW at a wavelength of 632.8 nm which is the reading beam. Various lens configurations were used to vary the spot size of the reading beam also.

The dichroic mirror allowed both beams to be incident from the same side onto the sample from the same side. This dichroic mirror reflects the longer red wavelengths while it passes the shorter blue or green wavelengths.

The sample wasa placed within an MMR Technologies Inc. model K-77 refrigerator which provided a temperature controlled environment for the sample. Sapphire windows on the refrigerator allowed the incident beams from the argon and HeNe lasers to illuminate the sample. By combining both Joule Thompaon effect cooling and separate heating of the sample, sample temperatures of between -30°C to +90°C were obtained.

The transmitted helium neon laser light is incident onto the MRD300 photodetector. The Motorola MRD 300 detector used to monitor the HeNe transmission through the photochromic sample used a load resistance of 1 kohm which gave a rise time of the detector of less than 1 μs. or a modulation frequency response of about 1 MHz.

This light passed through a 632.8 nm transmission filter which blocked any of the blue-green light from reaching the detector. The photodetector signal was recorded using Nicolet model 3091 digital oscilloscopes. In some cases, this oscilloscope was connected to an Apple IIe computer which recorded and allowed evaluation of the experimental data.

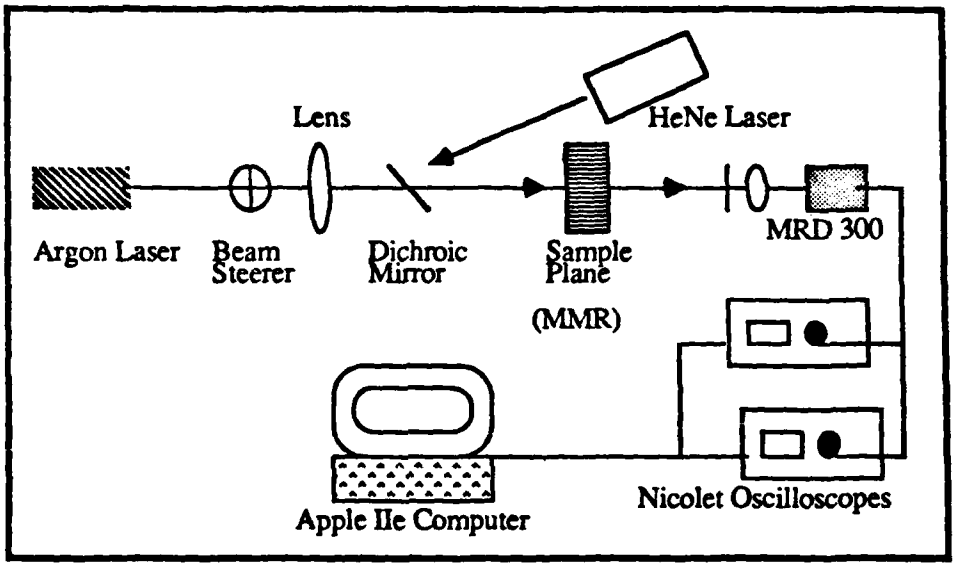

Figure 11. Schematic drawing of the low intensity relaxation experimental setup.

The general experimental approach common to all of the characterization experiments was to expose the photochromic samples with the argon write beam and measure the excited state concentration by monitoring the transmiossion of the read beam. However, since the excited state concentration depended on the intensity of the writing beam, care had to be taken to insure that the writing beam was spatially uniform over the size of the reading beam. As seen in Figure 11, the first step in achieving the uniform illumination and probing of the sample was the co-alignment of the argon and

HeNe laser beams. Direction of the beams was controlled with good quality beam steerers and lenses mounted in translation stages. A Newport Research Corporation model 675 beam steering device was used to direct the argon beam to a height comparable to the level of the sample plane. Lenses mounted in standard x-y and x-y-z translation stages were used throughout the setup to insure good positional control of the writing and reading beams. Once the argon beam was level and aligned in the approximate direction desired, the HeNe laser and a dichroic mirror were placed in the setup. The dichroic mirror directed the HeNe laser beam to the sample plane. The next step in achieving uniform illumination of the sample was to measure the write and read beam diameters and intensities at the sample plane.

Beam diameter and intensity measurements

Both the argon and HeNe lasers used throughout the experiments provided output in the fundamental, or TEM_{00} mode. The intensity profiles of the beams could thus be approximated using a Gaussian model as

$$I = I_0 \exp\{-2r^2 / a^2\} , \qquad (12)$$

where I_0 is given by $2P_t/\pi a^2$. The parameter a represents the beam's radius where the intensity is reduced to $1/e^2$ of the maximum value along the beam axis and r is the radius of the beam at some distance from the central axis. P_t represents the total output power of the laser.

The diameters of both beams were measured using an EG&G Reticon RL-256 scanning diode array detector. The detector is made up of 256 individual photodetectors aligned along a single row. The center to center spacing of the diodes is 25 μm. The Reticon diode array was connected to a Nicolet 3091 digital oscilloscope. The signal generated from individual detector elements was easily seen on the oscilloscope and the $1/e^2$ diameters of the argon and HeNe laser beams were measured to within ± 25 μm. The central region of the argon beam intensity represents the area of most uniform intensity. To insure that the HeNe beam accurately probed an area which was uniformly

written by the argon beam, the HeNe probe beam diameter was about one-fourth of the diameter of the argon write beam. This probe beam width corresponded to an intensity deviation from the central argon beam intensity peak of about 10%.

After the beam diameters (at the sample plane) were determined, the intensity of the central region of the argon beam at the sample plane was measured. In order to measure the power within the central area of the write beam, a circular aperture was placed at the sample plane. For the large, expanded beam used in the low intensity experiments, an aluminum disk with a 1 mm. hole was used in conjunction with the Newport Research Corporation model 820 detector to measure the power within the central area. Since the write beam diameter was smaller when using the higher intensity setups, a small pinhole capable of withstanding high energy input over an extended time period was required. A 100 μm. diameter gold-foil pinhole from Melles Griot was used for this purpose. One or two neutral density filters of OD 3 were used between the pinhole and the detector head, if needed. To calibrate the system, the laser power was raised in increments of 100 milliwatts and the power transmitted through the overall system and into the pinhole was recorded using the NRC model 820 power meter. The 1 cm^2 area NRC detector measures the total power which passes through the pinhole. By dividing the power reading from the detector by the area of the pinhole used to aperture the incident beam, the intensity at the sample plane was easily calculated. This method of measuring the sample plane intensity was quite reproducible from day to day with an associated error of about 5-10%.

When using the low and medium laser powers, the relationship between the argon laser output power and sample plane intensity was linear. As the laser output power doubled, the sample plane intensity also doubled. However, when using very high laser output power, the power meter reading at the sample plane was sometimes lower than anticipated since higher order Gaussian laser modes developed within the argon laser. The formation of the higher order mode was confirmed after exposing a photochromic

sample to a high intensity argon laser beam and noting that two small, slightly elongated spots of exposed photochromic sample were made, instead of the usual, single round spot. The two spots represent the formation of the TEM_{10} mode whereas the single round spot represents the fundamental TEM_{00} mode. Hence, to alleviate the problem of the reduced measured intensity at the sample plane, the output aperture of the argon laser was kept small and the output power of the laser was kept to a moderate level.

As discussed earlier, it is important in each of the experimental setups to have a uniform write beam intensity distribution across the photochromic sample target area to be probed. Many lens combinations can be used to achieve the desired result of a particular beam diameter at the sample plane depending on the writing intensity which was desired.

In the case of the low-intensity (10 - 50 mW/cm^2) setup, the 1.4 mm. diameter beam from the argon laser was expanded and collimated to a width of 4 cm.at the sample plane using a 5 cm. focal length negative lens and a 20 cm. focal length positive lens combination. The write beam fully covered the 8 mm. diameter sample aperture and led to a maximum intensity of 50 mW/cm^2 at the sample plane. Using this intensity, exposure of the samples containing photochromic material typically resulted in optical densities approaching 1.0 in a matter of several minutes. For this case, the origina $1/e^2$ diameter of the monitoring, or read, beam at the output of the HeNe laser was 0.9 mm. The read beam was expanded using a 5 cm. focal length negative lens placed 1 cm. from the output of the laser. The beam was collimated using a 15 cm. focal length positive lens placed approximately 15 cm. from the negative lens. The $1/e^2$ diameter of the read beam at the sample plane was about 8-10 mm. The intensity of the read beam at the sample plane was kept low (less than 2 mW/cm^2) in order to reduce the effect of optical relaxation enhancement as discussed in the previous chapter.

The the read beam transmitted through the sample aperture was collected by a 5 cm. focal length positive lens, passed through a 632.8 nm. narrow bandpass filter, and focussed onto the receiving lens of a Motorola MRD 300 photodetector.

Medium intensity experimental setup

Faster writing times were obtained using a different experimental configuration capable of writing intensities in the 10 -150 W/cm^2 range. The lens system used in the low intensity experiments was modified in order to increase the argon laser intensity at the sample plane. The sample plane was approximately 120 cm. from the argon-ion laser. The lens used for the write beam was a single 100 cm. focal length positive lens placed about 10 cm. from the output of the argon laser. This simple modification yielded a 1/e^2 beam diameter at the sample plane of 0.700 mm. $\pm$ 0.025 mm. The sample plane was 120 cm. from the front of the argon laser. Using this setup, the experimental range of intensities at the sample plane was 10 - 150 W/cm^2. For this configuration, the read beam needed to be focussed to a beam diameter of about one fourth the diameter of the write beam. A 20 cm. focal length positive lens was placed 15 cm. from the 5 cm. negative lens at the HeNe laser output. This combination yielded a 1/e^2 diameter of the read beam at the sample plane of 0.145 mm. $\pm$ 0.025 mm.

The shutter used to control the write beam exposure was a Newport Research Corporation model 845 mechanical shutter. This shutter had a minimum shutter time of 10 ms. and a rise time (10 - 90%) of about 650 μs. Since the device lacked an output trigger, the output of the shutter mechanism was modified to include a trigger line.

An improved technique for the control of the read beam included the use of Oriel model 18008 motorized micrometer stages. Each stage provided translation with a resolution of 0.1 micron. The stages were used along the x-z directions to hold the focussing lens of the read beam. Vertical, or y-direction displacement, was done with the use of a manually controlled micrometer .

Since the diameters of both the write and read beams were small, their images on the sample were difficult to see clearly with the unaided eye. A small telescope was made to view the target area. Final system alignment was begun by exposing the target area of the sample with the argon beam to produce a visibly darkened spot. The write beam, which was too intense to be viewed directly, was blocked while looking at the read beam striking the sample. A slight translation of the read beam's focussing lens then allowed the read beam to hit directly in the center of the practice spot made previously by the write beam. The sample was then translated on its mount to provide an unexposed target area for the write beam. The read beam detector's optics were moved to compensate for any read beam adjustments. Once this operation was done, the overall system alignment was quite stable and only minor adjustments were needed over the following hour or two.

High intensity experimental setup

Much higher writing intensities of 200 - 800 W/cm^2 at the sample plane were obtained using a different lens configuration. A 20 cm. focal length positive lens was used to focus the write beam to a 1/e^2 diameter of 0.300 mm. ± 0.025 mm. at the sample plane. The sample plane was 130 cm. from the output of the argon laser. The read beam was focussed using a 30 cm. focal length positive lens in conjunction with the 5 cm. focal length negative lens in front of the HeNe laser. The positive lens was placed 18 cm. from the negative lens and was 80 cm. from the sample plane. This led to a 1/e^2 diameter of 0.125 mm. ± 0.025 mm. at the sample plane. Although this diameter was not one-fourth the size of the write beam, it was the smallest beam size that could be attained with this setup.

Atttempts were made at obtaining higher writiing intensities. Substituting a 15 cm. focal length lens for the 20 cm. focal length lens in the high intensity setup just described produced a write beam diameter of about 0.10 mm. This small diameter led to a maximum argon laser beam intensity at the sample plane of over 1500 W/cm^2.

However, two things prevented the experimental use of this setup in the excitation of the photochromic samples. First, the requirement that the HeNe probe beam be about one-fourth the size of the argon write beam was difficult to realize experimentally. The minimum read beam diameter obtainable with this setup was about 0.080 mm. and this was much too large for the accurate monitoring of the photochromic reactions. Secondly, since the beam sizes were so small, the read beam striking the sample was very difficult to see even when using the observing telescope. Likewise, the tiny dark spot that the argon laser beam made on the sample was also extremely difficult to see. Co-alignment of the two beams was simply out of the question! Due to these problems, we decided to stay with the more-reliable 200-800 W/cm^2 range setup.

To reduce sample damage at these higher writing intensities, the beam was shuttered using an IntraAction Corporation (model AOM-40) acousto-optic light modulator, or AOLM. The AOLM has a rise time of 5 ns. and an effective minimum shutter speed of less than 10 ns. A BNC model 7010 Digital Delay Generator with output time ranging from 100 ns. to 99.9 sec., was used to gate the 40 MHz. driver of the AOLM. In this manner, optical pulses of 1 - 8 ms. were easily obtained.

Now that the experimental setups used in the characterization of the photochromic samples have been discussed, some of the properties of the polymer substrates which contain the photochromic molecules will be presented. The rest of this chapter describes the polymer matrix used as the substrate in this study.

Sample composition

Photochromic impregnated plastic film samples were obtained from Dr. Nori Chu, of the American Optical Corporation in Southbridge, Mass. The two species of photochromic molecules under study were mercury bis-dithizonate and phenyl mercury dithizonate (samples I - IV). The experimental results of this project indicated that the mercury bisdithizonate samples had a faster writing time than did the phenyl mercury dithizonate samples. With this in mind, more samples of mercury bisdithizonate

(samples V1 - V6) were obtained from American Optical Corporation. Table 1 indicates the number designator, sample composition and thickness of the samples used throughout the experiments.

Table 1. Composition and Thickness of Photochromic Samples

Number	% Photochromic Material	Thickness (mm.)
I	0.2% mercury bisdithizonate	0.178
II	0.4% mercury bisdithizonate	0.178
III	0.26% phenyl mercury dithizonate	0.178
IV	0.53% phenyl mercury dithizonate	0.178
V-1	no photochromic material	0.178
V-2	0.2% mercury bisdithizonate	0.178
V-3	0.5% mercury bisdithizonate	0.178
V-4	1.0% mercury bisdithizonate	0.203
V-5	1.0% mercury bisdithizonate	0.279
V-6	1.0% mercury bisdithizonate	0.406

Cellulose acetate butyrate. The plastic film used as the substrate for the photochromic molecules was cellulose acetate butyrate, or CAB which is a cellulose-based polymer used in transparent plastic applications (11). Refer to Table 2 for specifications regarding CAB (12,13). The cellulostic fibers of the plastic are intertwined in a random fashion (14) and the photochromic molecules are situated between and at the ends of adjacent polymer chains. The molecules are not chemically attached to the polymer backbone but lie within the matrix are presumed to be randomly distributed throughout the plastic material. The photochromic molecules may be found in distinct regions of the polymer matrix. These regions include the volume between adjacent

Table 2. Cellulose acetate butyrate properties

Index of refraction	1.46 - 1.49
Mass density	1.25 g/cm^3
Specific heat	0.3 - 0.4 cal/g^{o}C

polymer strands and the volume between the ends of the polymer strands. The common use of additives to the plastic to increase its pliability, surface hardness, atmospheric stability and other factors (14) are present in small amounts and are presumed not to interfere appreciably with the photochromic reactions.

The experimental techniques and components used to characterize the photochromic process in plastic samples containing two different species of mercury dithizonate molecules have been presented. The rest of this report contains the experimental observations which were obtained as a result of these experimental techniques. First, UV-visible spectral profiles of the photochromic samples are

presented in the next chapter. Following the spectral absorbance discussion, the remainder of this report will present and discuss the experimental results which were obtained from the photochromic excitation and relaxation experiments.

Chapter IV - Optical Spectra of Ground and Excited States of Mercury Bisdithizonate and Phenyl Mercury Dithizonate

Visible-Ultraviolet Spectra

Optical absorbance spectra of CAB polymer samples containing mercury bisdithizonate and phenyl mercury dithizonate were obtained to see if the absorbance profiles of the polymer-photochrome systems differed significantly from those of the photochromic species in solution form. Since the photochromic molecules are not attached to the polymer backbone, no large changes in the absorption profiles between the solution form and the plastic matrix form of the photochromic molecules were expected. Absorbance spectra in the ultraviolet and visible spectral ranges for the ground and partially activated states of the photochrome-polymer systems were obtained using a dual beam Perkin-Elmer 555 spectrophotometer. The spectral range of the scans was 250 - 800 nm. Throughout the scans, visual inspection showed no signs of excitation of the photochromic species due to the scanning light probe.

Figure 12 shows the general spectral features of the mercury bisdithizonate-polymer system (sample I). The curves are redrawn from the original spectra and superimposed on the same plot (and are for qualitative use only). The very strong absorption peak of the unilluminated sample containing 0.2% mercury bisdithizonate gave an absorbance (or optical density) of over 3.0 at a central wavelength of 485 nm. The full-width at half-max (FWHM) range was approximately 100 nm. There was no detectable absorbance in the 580 - 800 nm. range. The central wavelength of 485 nm. agrees precisely with that reported for mercury bisdithizonate dissolved in solutions of

either chloroform ($CHCl_3$) or carbon tetrachloride (CCl_4) (3). The partial excitation of this sample with low intensity white light for 10 minutes led to a decrease in the

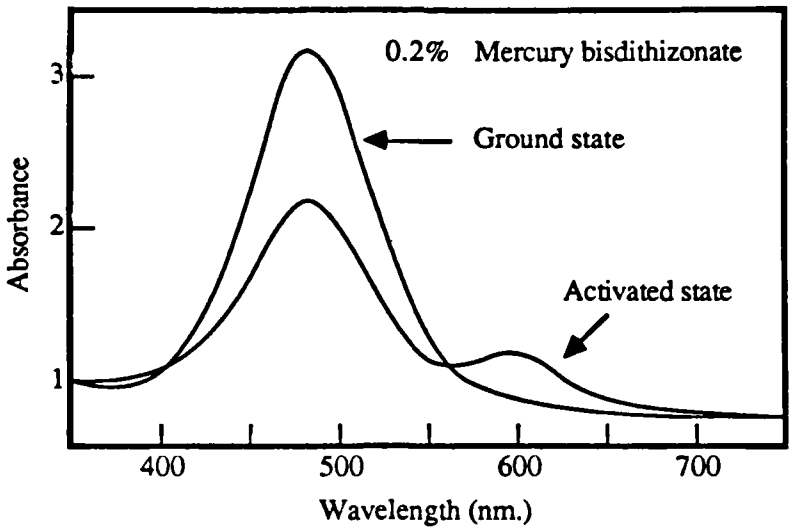

Figure 12. Qualitative absorbance spectra of the mercury bisdithizonate sample (sample I) used in this study.

absorbance at 485 nm., and a developing peak at 600 nm. The peak at 600 nm. was weak since the illumination of the sample had been of low intensity and short duration.

Figure 13 shows the general spectral features of the phenyl mercury dithizonate-polymer system (sample III). The major absorption peak of the unilluminated sample containing 0.26% phenyl mercury dithizonate is at 475 nm. with a FWHM of approximately 80 nm. This peak represents an absorbance of about 2, considerably less than the > 3.0 absorbance peak of the 0.2% mercury bisdithizonate sample. The central wavelength of 475 nm. agrees well with that reported for phenyl mercury dithizonate dissolved in chloroform ($CHCl_3$) (3). Low intensity illumination of the phenyl mercury dithizonate sample led to a decrease in the peak at 475 nm. with a developing peak centered on 588 nm. As in the previous case, this new peak is weak because of the low intensity illumination of the sample.

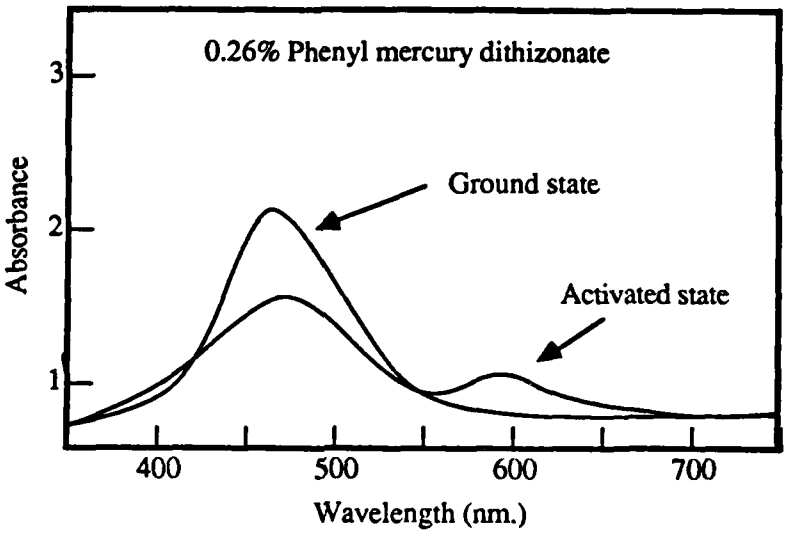

Figure 13. Qualitative absorbance spectra of the phenyl mercury dithizonate sample (sample III) used in this study.

The difference in the relative absorbances (around 480 nm.) of the mercury bisdithizonate and phenyl mercury dithizonate samples is real and not a consequence of the difference in the percent concentrations of photochromic species used. The molecular weight of phenyl mercury dithizonate is 521 gm. and the molecular weight of mercury bisdithizonate is 687 gm. The ratio of the molecular weights is 1:1.13. The different percent concentrations (by weight with respect to the plastic) of the samples reflects the fact that a 0.2% mercury bisdithizonate sample contains the same number of molecules as a 0.26% sample of phenyl mercury dithizonate, but has twice the number of photochromic ligands. Further support of the observed larger optical density of the mercury bisdithizonate over that of the phenyl mercury dithizonate is found in the literature. Hutton and Irving have reported extinction coefficients for chloroform solutions of mercury bisdithizonate and phenyl mercury dithizonate of 7050 m^2/mole (λ_{max} = 480 nm.) and 3500 (λ_{max} = 475 nm.) m^2/mole, respectively (15). As was

found in this work, the one-ligand species is only about half as absorbing as the two-ligand species at their ground state absorbance maxima.

Molar absorptivity curves of mercury bisdithizonate [$Hg(HDz)_2$], single-ligand mercury dithizonate [HgHDz], and dithizone [H_2Dz] in benzene solutions (16) (which may be present in small concentrations in the plastic samples) show absorbance profiles which are similar to those of the mercury bisdithizonate and phenyl mercury dithizonate molecules used in this study. Their presence in the samples may affect the observations of the photochromic reactions associated with the mercury bisdithizonate and phenyl mercury dithizonate components. The major peaks of the secondary mercury (I) and (II) dithizonate species are shifted to the 490 - 520 nm. region. The term secondary refers to the dual bonding of the dithizone molecule to the metal due to the loss of two hydrogen atoms from the ligand. The major ground peak of the ligand itself, dithizone, is around 445 nm. while the highly absorbing activated peak is around 610 nm.(4).

The absorbance profiles of the photochromic plastic samples used in this work are essentially the same as those associated with the photochromic molecules in solution form. These observations support the idea that the photochromic molecules are not chemically bound to the polymer chains but lie between and at the ends of the plastic strands. Thus, the excitation and relaxation of the polymer-bound photochromic molecules should occur in a similar manner as observed in a solution of the photochromic compounds. However, since the plastic matrix represents a more viscous environment than either the chloroform or carbon tetrachloride liquids, the isomerization of the photochromic molecules would be expected to be slower in the plastic matrix than in the liquids. The next chapter will examine the general photochromic behavior of polymer-bound mercury bisdithizonate and phenyl mercury dithizonate molecules.

Chapter V - General Experimental Behavior of Photochromic Materials

As discussed in the preceding chapters, the behavior of photochromic systems is complex. The observed rates of the excitation and relaxation reactions depend on photochromic species and concentration, incident write light intensity and wavelength, read beam intensity, and sample temperature. Each of these parameters affects the photochromic process in a particular manner. For example, the rates of the excitation and relaxation reactions increase when the sample temperature increases. Also, an increase in the incident write beam intensity leads to an increase in the rate of the excitation reaction. In order to gain some qualitative insight into the photochromic process, a plastic sample containing mercury bisdithizonate was exposed to a write beam under some extreme conditions of sample temperature and the excitation and relaxation processes were observed.

Figure 14 shows the transmitted HeNe intensity versus time for the writing and relaxation cycles of a sample containing 0.2% mercury bisdithizonate when exposed to a low write beam intensity of 10 W/cm^2 (λ = 488.0 nm.). Three curves are drawn, each one representing the normalized transmitted HeNe intensity as a function of time for a given sample temperature. The top curve is for a sample temperature of 135°C. The middle and lower curves correspond to sample temperatures of 100°C and 25°C, respectively. The large range of temperatures was obtained using a hot-air gun to warm the sample inside an enclosed volume. This method of heating worked well but the movement of the air from the hot air gun caused rapid movements in the sample as well. Consequently, there were flucuations present in the HeNe intensity transmitted through the sample. Hence the results are suitable for qualitative discussion, but are not designed to be explicitly quantitative in nature. Experimentally, the sample was exposed to the

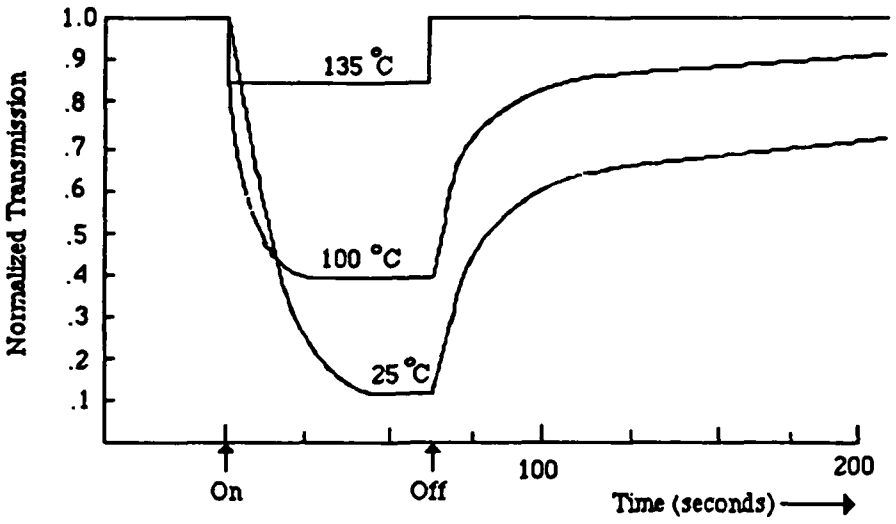

Figure 14. Writing and relaxation cycles for 0.2% mercury bisdithizonate at 25°C, 100°C, and 135°C.

incident write beam intensity until optical saturation of the read beam occurred. Once optical saturation was evident, the write beam was turned off and the photochromic system was allowed to relax. A qualitative discussion of the observations follows.

At a sample temperature of 135°C, optical saturation of the sample was reached in a very short time. However, the saturated optical density was a very low value of 0.07 and is a result of competition between the excitation and relaxation reactions. The optically-induced excitation reaction results in the rapid formation of excited state molecules and in the rapid absorption of the HeNe read beam. However, since the relaxation reaction rate constant follows a temperature-dependent Boltzmann distribution, the relaxation reaction at a high temperature causes de-excitation of the excited molecules as quickly as they are formed. The rapid formation and depletion of the excited state photochromic molecules within the polymer matrix results in a small equilibrium concentration of excited molecules. Thus, the absorbance of the 632.8 nm. HeNe monitoring beam at equilibrium is relatively low. Once the writing beam is turned

off, no further excitation of the ground state molecules occurs. The excited molecules continue to thermally relax to the ground state. Since the sample temperature is relatively high, the relaxation occurs rapidly and the HeNe read beam transmission rises very quickly to its original level. Therefore, the behavior of a photochromic sample at 135°C includes a rapid writing and relaxation cycle, with a shallow optical density resulting at equilibrium.

At a lower sample temperature of 100°C, the writing time to saturation is longer than that observed in the 135°C setup, and the depth of the optical density at saturation is much greater. The increase in the depth of the optical density is a result of the decrease in the competition between the excitation and relaxation reactions of the photochromic molecules. The decrease in competition occurs because the lower temperature leads to a lower relaxation rate constant, which, in turn, leads to a longer relaxation time. The continual de-excitation of the excited molecules therefore occurs more slowly, and the concentration of excited molecules at equilibium is greater in this case than it was in the previous, higher temperature case. Once the excitation light is turned off, the excited molecules thermally relax to the ground state, but at a lower rate than in the previous case.

Lowering the sample temperature to 25°C further illustrates the decrease in the competition between the excitation and relaxation reactions. As the temperature decreases, the excitation reaction rate modestly decreases. The decrease in the HeNe read beam transmission upon illumination of the sample with the write beam is not as rapid as it was in the previous cases. This effect illustrates the temperature dependence of the forward reaction. In addition, the optical density at equilibrium is greater than in the two previous cases. The increase in the optical density reflects the increase in the concentration of the excited state molecules at equilibrium which is due to the decrease of the relaxation rate of the return reaction. As was discussed previously, the relaxation rate constant follows a Boltzmann distribution and hence a decrease in the temperature

leads to a decrease in the reaction rate. The competition between the excitation and relaxation reactions is therefore decreased at this sample temperature and the equilibrium concentration of excited molecules becomes relatively large. After the write beam is turned off, the relaxation of the excited molecules occurs more slowly at this temperature than was previously observed at the higher temperatures. Hence, at a sample temperature of 25°C, the optical density at saturation is greater than the optical density observed at saturation for a sample temperature of either 100°C or 135°C and the relaxation reaction occurs more slowly.

This overview of the temperature dependence of the photochromic system provides an understanding of the general behavior of the photochromic process. Underlying the process is the fact that photochromic molecules are being transformed between two states. This transformation of the molecules is the result of both optical and thermal mechanisms. The primary driving-force of the forward excitation reaction involves the optically-induced excitation of ground state photochromic molecules. As observed in the previous figure, the excitation reaction is also temperature-dependent. The depth of the optical density (at 632.8 nm.) generally decreases as the sample temperature increases due to competition between the excitation and relaxation reactions. On the other hand, the relaxation reaction involves a thermal mechanism as the primary decay route for the excited molecules. In the absence of the activating blue-green light, the relaxation of the excited molecules increases as the temperature increases. Both the optical activation and the thermal relaxation mechanisms were discussed earlier using the potential energy diagrams associated with the photochromic reactions.

An optically-induced mechanism may or may not be involved (depending on the photochromic species) as a secondary relaxation route. This optically enhanced relaxation of the excited molecules was discussed briefly in Chapter II. By experimentally keeping the read beam intensity relatively low, this secondary relaxation route is effectively minimized. Thus, the two relaxation mechanisms can be

experimentally decoupled. This decoupling allows one to investigate either the thermal or the optical dependence of the relaxation reaction. The optically enhanced relaxation reaction was not investigated in this work. However, the temperature dependence and kinetics of the relaxation reaction were studied in detail and are discussed in the following chapter.

Chapter VI - Kinetics of the Relaxation Reaction

The previous chapter provided an introduction to the general temperature dependent photochromic behavior of polymeric CAB samples containing mercury bisdithizonate molecules. For a given incident write beam intensity, the number of excited molecules which are present at equilibrium depends on the temperature of the sample. The number of excited molecules at equilibrium decreases as the temperature increases due to an increase in the rate of the relaxation reaction. The increase of the relaxation rate means that there is an increase in the number of transitions from the excited state to the ground state which results in less absorption of the read beam. Hence, at relatively high temperatures (and a moderate write beam intensity), the equilibrium optical density is quite low. However, as the temperature decreases, the relaxation rate decreases and the number of excited molecules at equilibrium is not depleted as rapidly. At a lower temperature, the equilibrium concentration of excited molecules is relatively high and one observes an increase in the equilibrium optical density of the photochromic material.

Since both the excitation and relaxation reactions of the photochromic molecules occur concurrently in the presence of the write beam, one must isolate the relaxation reaction of the excited molecules in the absence of the write beam. The remainder of this chapter will examine the relaxation reaction kinetics of the excited state photochrome-polymer system after the write beam has been turned off. The rate constants and activation energies for the relaxation reactions of the two species of photochromic molecules used in this work will be presented and discussed.

Thermal relaxation experiments

Samples containing 0.2% and 0.4% mercury bisdithizonate and 0.26% and 0.53% phenyl mercury dithizonate were exposed to an incident write beam (λ = 488.0 nm.) intensity of 50 mW/cm^2 and allowed to reach optical saturation. The write beam was then turned off and the relaxation reaction was followed by monitoring the increase in the transmission of the HeNe read beam intensity. The incident HeNe read beam intensity was 1 mW/cm^2. The sample temperatures were 10°C, 50°C, and 90°C. The experimental setup used was the low-intensity setup described in Chapter III. The following section discusses the primary results obtained from the experiments.

Figure 15 shows the HeNe read beam transmission vs. time for the relaxation of a sample containing 0.2% mercury bisdithizonate at 10°C. Note that after 100 minutes had elapsed from the removal of the write beam, the transmitted intensity had reached roughly 40% of the original read beam transmission. In contrast, Figure 16 shows the HeNe read beam transmission vs. time for the relaxation of 0.2% mercury bisdithizonate at 90°C. In this case, the transmitted HeNe beam had returned to better than 90% of the original intensity after about 50 minutes. The increase in sample temperature allowed for the faster relaxation of the excited state mercury bisdithizonate molecules to the ground state.

Figures 17 and 18 reflect a similar temperature dependence of the relaxation reaction for samples containing phenyl mercury dithizonate. Figure 17 shows the HeNe read beam transmission vs. time for the relaxation of a 0.26% phenyl mercury dithizonate sample at 10°C. After reaching a minimum HeNe read beam transmission of about 10%, the throughput increased to only 25-30% after 100 minutes. Figure 18 shows the HeNe read beam transmission vs. time for the relaxation of a 0.26% phenyl mercury dithizonate sample at 90°C. The plot shows that after only 25-30 minutes of relaxation time, the HeNe transmission was back to better than 90% of the original value. In each of these cases, the minimum transmission was about 10%.

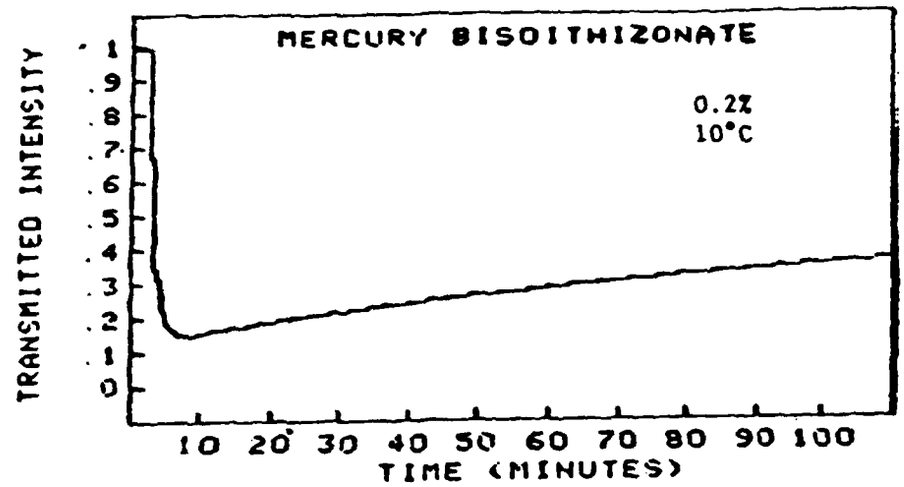

Figure 15. Transmitted HeNe read beam intensity vs. time (minutes) for the writing and relaxation cycle of 0.2% mercury bisdithizonate at 10°C.

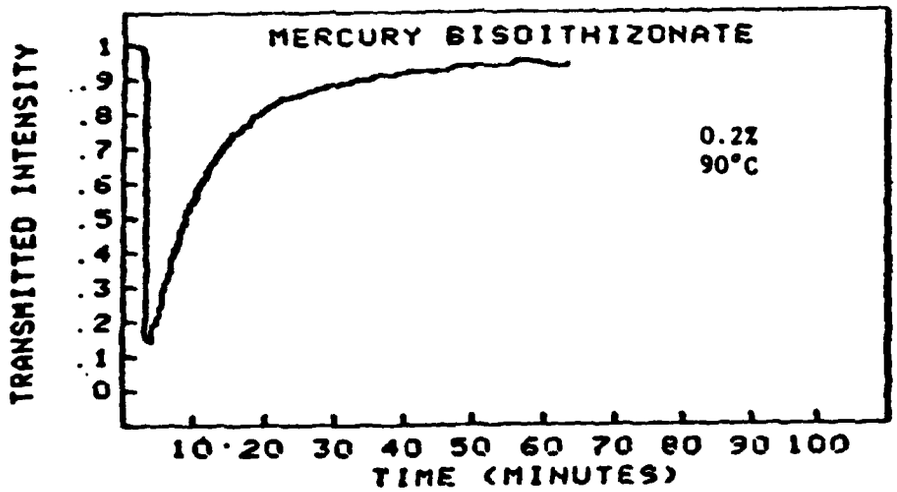

Figure 16. Transmitted HeNe read beam intensity vs. time (minutes) for the writing and relaxation cycle of 0.2% mercury bisdithizonate at 90°C.

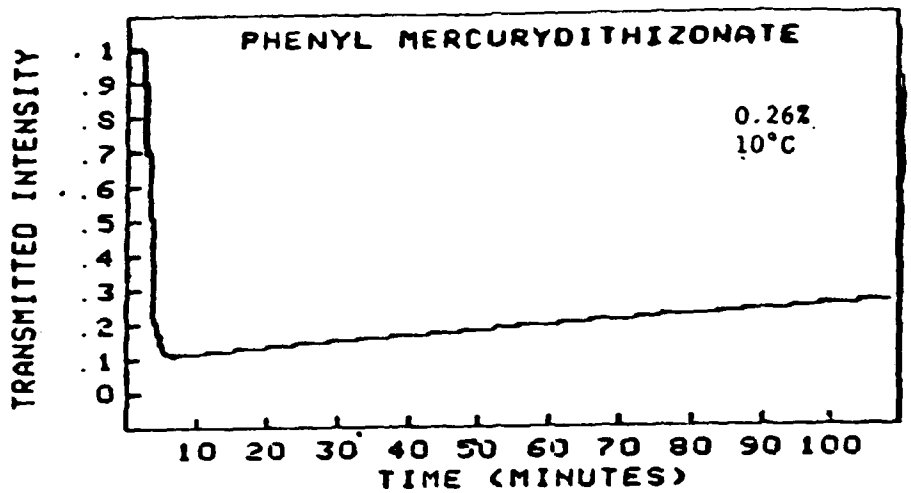

Figure 17. Transmitted HeNe read beam intensity vs. time (minutes) for the writing and relaxation cycle of 0.26% phenyl mercury dithizonate at 10°C.

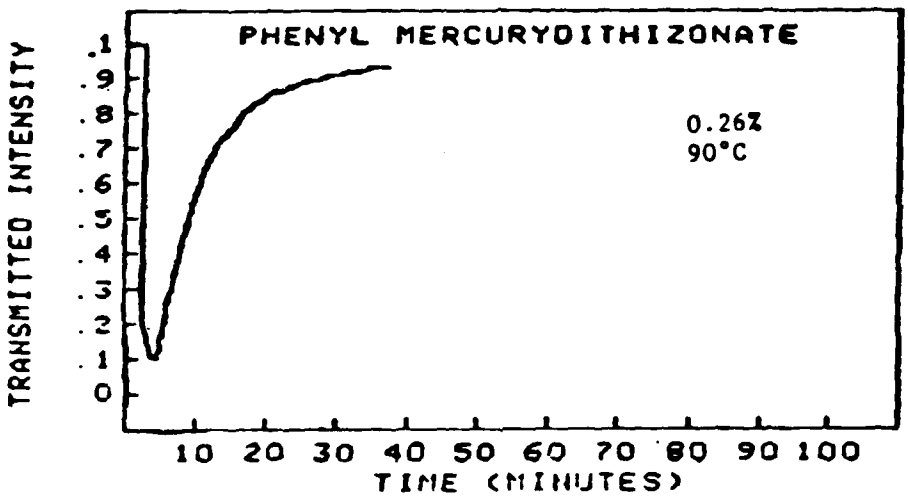

Figure 18. Transmitted HeNeread beam intensity vs. time (minutes) for the writing and relaxation cycle of 0.26% phenyl mercury dithizonate at 90°C.

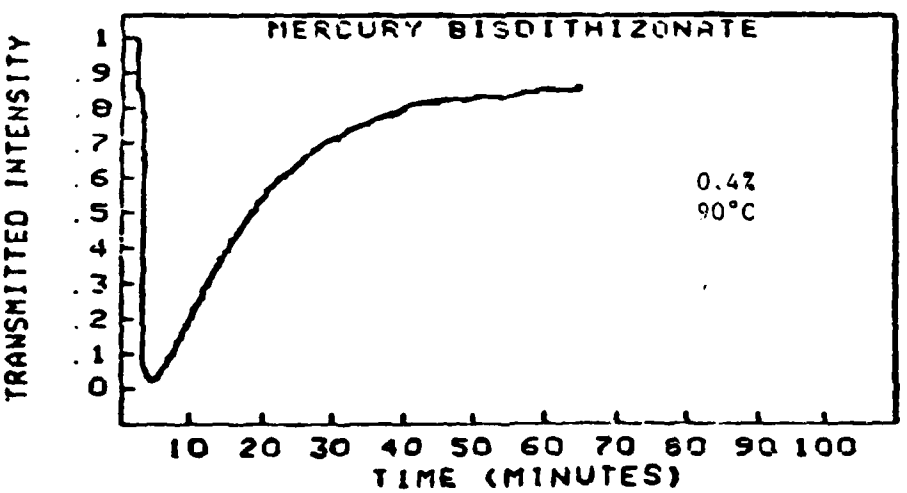

Figure 19. Transmitted HeNe read beam intensity vs. time (minutes) for the writing and relaxation cycle of 0.4% mercury bisdithizonate at 90°C.

We also investigated the dependence of the relaxation reaction on the photochrome concentration. Figure 19 shows the HeNe read beam transmission vs. time for relaxation of a sample containing 0.4% mercury bisdithizonate at a sample temperature of 90°C. The plot shows that after about 50-60 minutes of relaxation time, the transmission had returned to about 85% of its original value. Comparison of this figure with Figure 16 (.2% mercury bisdithizonate) reveals two pertinent observations. First, for the same temperature and material, the 0.4% concentration had a slightly lower minimum transmission level than did the 0.2% concentration for the same exposure time to the write beam. The minimum transmission of the 0.4% sample was about 1-2% while the minimum transmission of the 0.2% sample was about 15%. This seems reasonable since the sample containing the higher concentration has more photochromic molecules with which to absorb the incident read beam. Secondly, the relaxation of the excited molecules of the higher concentration appears to occur a bit slower than that of the lower concentration sample. This behavior is not expected if the relaxation reaction follows first-order kinetics, since the relaxation of the excited state should occur independently of the initial concentration. The following section provides a detailed analysis of the data concerning the kinetics of the relaxation reaction.

Determination of the rate constant and activation energy of the relaxation reaction

The relationship of the optical density of the exposed photochromic samples to the relaxation time was found in Equation (8) and the results from the previous section may be re-plotted and several system parameters evaluated. This section will discuss the methods used to evaluate the temperature-dependent rate constants and the activation energy of the relaxation reactions corresponding to the polymer-bound mercury bisdithizonate and phenyl mercury dithizonate species.

Figures 20 and 21 show semi-logarithmic plots of the optical density versus time for the relaxation reactions of samples containing 0.2% and 0.4% mercury bisdithizonate (samples I and II) at various temperatures. Figures 22 and 23 show

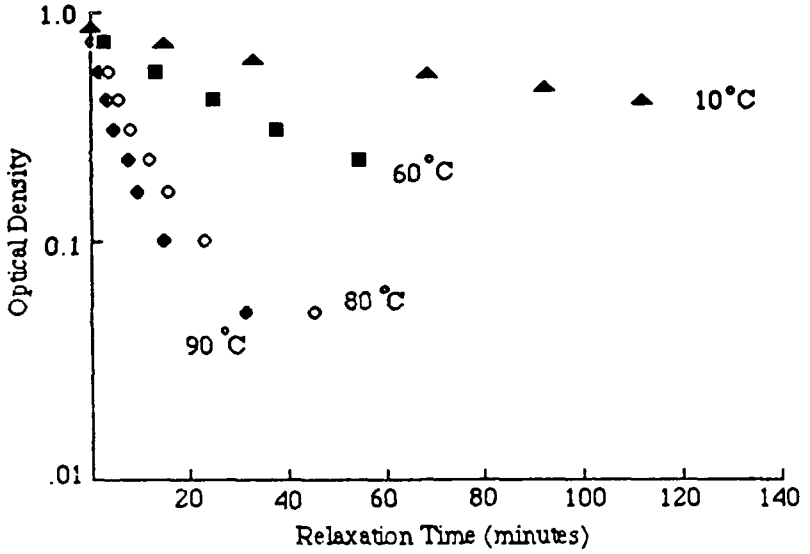

Figure 20. Optical density versus relaxation time (min.) at various sample temperatures for 0.2% mercury bisdithizonate (sample I). Key: closed diamond, 90°C; open diamond, 80°C; closed square, 60°C; closed triangle, 10°C.

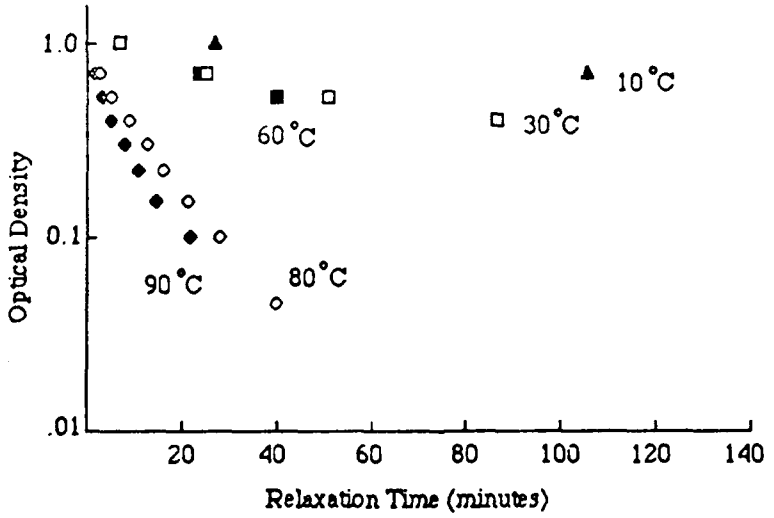

Figure 21. Optical density versus relaxation time (min.) at various sample temperatures for 0.4% mercury bisdithizonate (sample II). Key: closed diamond, 90°C; open diamond, 80°C; closed square, 60°C; open square, 30°C; closed triangle, 30°C.

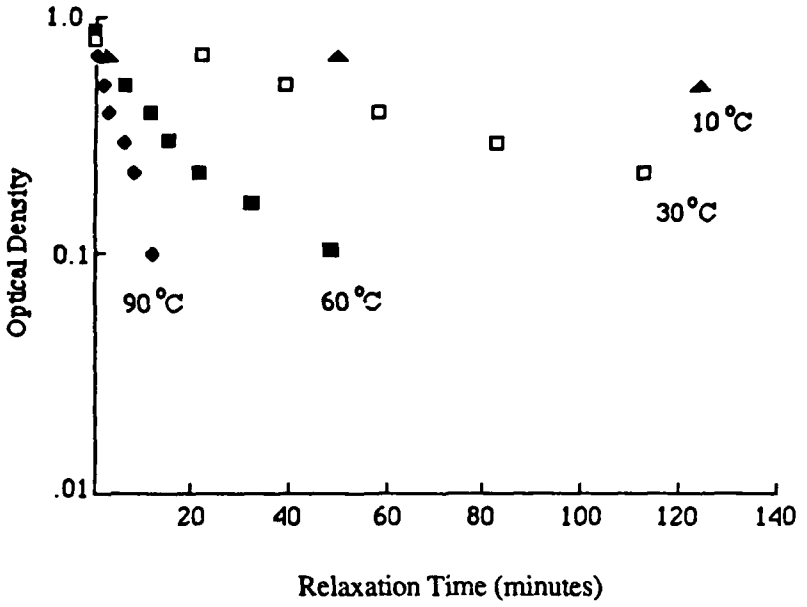

Figure 22. Optical density versus relaxation time (min.) at various sample temperatures for 0.26% phenyl mercury dithizonate (sample III). Key: closed diamond, 90°C; closed square, 60°C; open square, 30°C; closed triangle, 10°C.

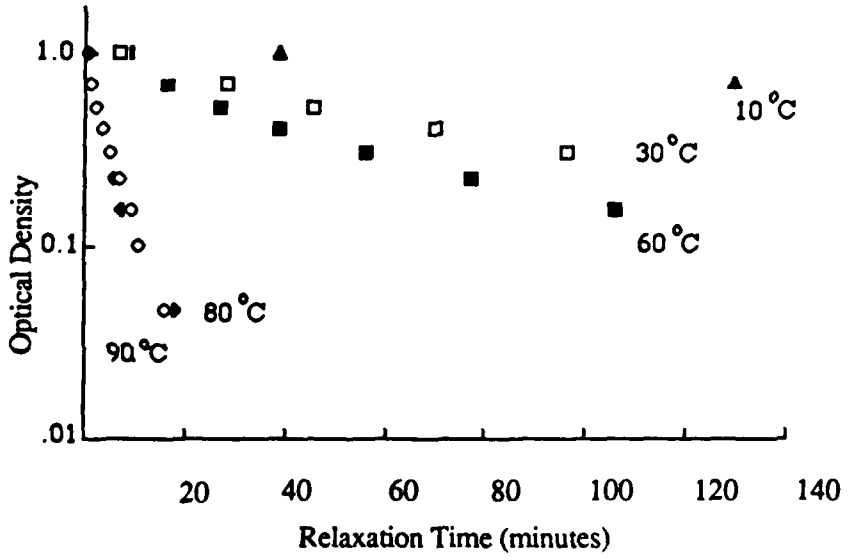

Figure 23. Optical density versus relaxation time (min.) at various sample temperatures for 0.53% phenyl mercury dithizonate (sample IV). Key: closed diamond, 90°C; open diamond, 80°C; closed square, 60°C; open square, 30°C; closed triangle, 10°C.

similar plots for the relaxation reactions of samples containing 0.26% and 0.53% phenyl mercury dithizonate (samples III and IV). The semi-logarithimic plots should reveal a linear relationship between the logarithm of the optical density and time as was discussed in Equation (8) of Chapter II. This linearity is present to some extent in all of the plots. However, the data from some of the higher temperature runs show a slight departure from linearity after the first few minutes of the relaxation reaction. This is due, in part, to the experimental error associated with the reduction of the HeNe read beam transmission data taken late in the relaxation reaction. There was considerable scatter in the data once the relaxation reaction had returned to about 80% transmission. The plots showing the relaxation behavior of the system at lower temperatures do not show this non-linearity on the time scale used because the return reaction had not evolved far enough along to show much scatter in the data.

There are other possible explainations for the non-linear behavior. As stated in Chapter II, if more than one photochromic species is present in the samples, then a semi-logarithmic plot of the optical density versus time may appear non-linear. This effect would be due to two (or more) species absorbing the HeNe probe intensity during different times of the relaxation reaction. Dithizone, the parent compound from which the mercury dithizonates are derived, may be present in small amounts in the polymer-photochrome system. Ground state dithizone absorbs in a similar blue-green region of the visible spectrum as the mercury dithizonate compounds. Dithizone is promoted to its excited state when the polymer-photochrome system is exposed to an incident excitation beam. The excited state molecules of dithizone absorb around 620 nm., which is close to the major absorption wavelengths of the mercury dithizonate compounds and the HeNe laser wavelength. Since the excitation of the photochromic molecules within the polymer matrix is dependent on both the temperature and the incident write beam intensity, it is difficult to decouple the excitation of the dithizone molecules from the excitation of the mercury dithizonate compounds. However, since the relaxation reaction

is studied in the absence of the incident write beam, the thermal relaxation of the system may be used to distinquish the relaxation of the dithizone molecules from that of the mercury dithizonate molecules if the species have different relaxation constants. The different relaxation rates of the photochromic species will result in a non-linear slope of the plot of the semi-logarithmic relationship between the optical density and the relaxation time.

Another property of the polymer-photochrome system which may lead to a non-linear log OD vs. time relationship is the physical structure of the polymer matrix. This structural effect depends on the relative sizes of the photochromic molecules and the volume available for their occupation within the polymer matrix. Studies have indicated that some plastics have different local environments within the polymer matrix in which photochromic molecules may reside (17). The local environments differ mainly in the volume available for the isomerization of the photochromic molecules. The occupation by the photochromic molecules of the relatively large volume at the ends of the polymer chains allows for easy physical isomerization of the photochromic molecules. This would lead to a larger rate constant for the relaxation reaction. On the other hand, occupation by the photochromic molecules of the relatively smaller volume present between adjacent polymer strands would tend to inhibit the relaxation isomerization of the excited molecules. This effect would lead to a smaller rate constant for the relaxation reaction. However, the continual thermal agitation of the polymer matrix is constantly changing the local environment of any particular photochromic molecule. Thus, the reaction rates associated with excited photochromic molecules within these types of polymers will depend on the average local environment of the polymer which is available for the photochromic molecules. Krezsylewski and coworkers showed that, upon warming plastic samples (those types which displayed the two rate behavior) containing photochromic molecules to a temperature above the glass transition temperature of the plastic, a single rate constant (in close agreement with the larger rate

constant found for the case of $T < T_g$) was obtained (17). They interpreted this effect to mean that the increase in thermal energy of the matrix (due to a high sample temperature) caused an increase in the kinetic motion of the polymer strands. This increase in the polymer motion increases the probability that any particular photochromic molecule will combine with a relatively large volume, thereby increasing the rate of isomerization of the excited molecule.

The previous discussion was presented to explain why some non-linear behavior might be present in the relaxation results. However, the results contained in this work do not show extreme deviation from first-order linear behavior. The slopes of the previously described plots are linear within (at least) the first minutes of the relaxation reaction. Hence, the dependence of the observed rates on the sample temperature and reactant concentration will be treated as if the system obeys (pseudo) first order kinetics.

Determination of the rate constant of the relaxation reaction. From Equation (8), the relaxation constant, k, may be calculated from the slope of the plot of the log of the OD vs. time. The experimentally observed relaxation reaction rate, k, was determined from the slope of the initial part of the experimental relaxation plots. Table 3 lists the rate constants for the samples containing 0.2% and 0.4% mercury bisdithizonate (I and II) and the samples containing 0.26% and 0.53% phenyl mercury dithizonate (III and IV) for various temperatures. For the 30 - 90°C (303 - 363 K) temperature range, the single-ligand species has a larger relaxation rate constant than does the dual-ligand species. This indicates that the excited single-ligand phenyl mercury dithizonate species isomerizes to the ground state faster than the dual-ligand mercury bisdithizonate species. The slower relaxation rate of the mercury bisdithizonate may mean that less competition occurs between the excitation and relaxation reactions of the dual-ligand species. However, at 10 - 30°C (283 - 303K), the rate constants of the two differentconcentrations of the phenyl mercury dithizonate (samples III and IV) are essentially equal to or slightly less than the relaxation rates of the two concentrations of

Table 3. Relaxation rate constants (k) for CAB-film samples of mercury bisdithizonate and phenyl mercury dithizonate (samples I through IV).

Temperature (K)	1/T (10^3 K^{-1})	k_I	k_{II}	k_{III}	k_{IV}
		(x 10^5 sec^{-1})		(x 10^5 sec^{-1})	
363	2.75	110	109	-	260
353	2.83	82.1	66.6	182	160
333	3.00	17.2	13.6	29.8	21.3
303	3.30	-	8.0	9.0	10.7
283	3.53	<4.47	3.3	2.67	2.12

mercury dithizonate (samples I and II). The similarity in the rate constants of each species at these lower temperatures indicates that the relaxation reactions of the excited states of each species are occurring at a similar speed, within experimental error.

One might expect that the relaxation reaction rates for each of the species at all sample temperatures should be in close agreement. Meriwether has suggested that the isomerism rate of excited state mercury dithizonate molecules in solution is independent of the number of ligands attached to the central mercury atom (5). This might further suggest that the isomerization reaction of the mercury dithizonate molecules in the plastic should also be independent of the number of ligands attached to the mercury atom. The experimental observation that the rate constants for each of the species examined in this work do not match is not necessarily in direct contrast to Meriwether's statement, but does support the supposition that the polymer matrix hinders the relaxation reaction of the photochromic molecules. In addition, the similar rate constants of the different species at sample temperatures below 30°C may be the result of a temperature-dependent decrease in the thermal motion of the polymer strands. At a relatively low sample temperature, the decrease in the thermal motion of the polymer chains which surround

the photochromic molecules would result in an increase of the steric hindrance of the isomerization reaction of the excited molecules. If the decrease in the polymer chain thermal motion is significantly large, then both the dual-ligand molecule and the single-ligand molecule will be appreciably hindered in their ability to isomerize. Thus, the rate constants for the relaxation of both the single and dual-ligand mercury dithizonate species in a low temperature polymer matrix may be similar.

The observed values of the mercury bisdithizonate rate constants at sample temperatures of 10°C and 30°C (approximately 3 - 8 x 10^{-5} sec^{-1}) are in general agreement with the rate constant of 21 x 10^{-5} sec^{-1} at 15°C reported for a polymer of mercury bisdithizonate (p-acetamidophenyl mercuric diphenylthiocarbazonate) blended with a polystyrene polymer substrate (18).

Benzene solutions of mercury bisdithizonate, which allow for a large amount of molecular movement, provide even larger relaxation rate constants. Meriwether and coworkers report that for a dry 14 μM benzene solution of mercury bisdithizonate at 25°C, the rate constant for the relaxation reaction is 130 x 10^{-5} $sec.^{-1}$ (5). The presence of 0.039 M H_2O in a 12.6 μM benzene solution of mercury bisdithizonate increased the relaxation rate constant to 1940 x 10^{-5} $sec.^{-1}$. According to Meriwether, the water molecules may provide a proton bridge between themselves and the photochromic molecules. The proton bridge enhances the proton transfer required for the isomerism of the excited state molecule to the ground state. Comparison of the values reported for the relaxation reaction of mercury bisdithizonate in benzene to the 8 x 10^{-5} $sec.^{-1}$ value for the relaxation rate constant obtained in this study for 0.4% mercury bisdithizonate (in CAB) at 30°C, leads to the observation that the relaxation reaction occurs about 15 - 240 times faster in a benzene solution (depending on the water content) than it does in the CAB plastic polymer.

The lower rate of relaxation of the excited molecules in the CAB plastic matrix is due to at least two phenomena. First, as previously discussed, the relative rigidity of the

polymeric chains within the plastic makes any type of molecular rearrangement more difficult than when the molecules are in a non-rigid, liquid medium. Second, in light of Meriwether's comment on the possibility of water molecules acting as proton bridges in the transfer of protons in benzene solutions of photochromic molecules, the question of a similar mechanistic device occurring in the plastic sample may be raised.

To study such a proton-bridge mechanism in the case of photochromic-impregnated polymers, one might incorporate a small amount of deuterated water (or, more directly, deuterated polymer) into the photochrome-plastic system and expose the system to an excitation write beam. After several excitation and relaxation cycles, the polymer could be dissolved and the photochromic molecules spectroscopically analyzed. A study of the infrared absorbance profile of the photochromic molecules (in particular, the N-H stretch bonds which are formed during the isomerization of the molecules) would indicate whether or not they had acquired any of the deuterium. The ground state N-H stretch of the dithizonate ligand in a molecule of mercury bisdithizonate is 3280 cm^{-1} (3340 cm^{-1} in the activated state) wheras the ground state N-D stretch is about 2400 cm^{-1} (2470 cm^{-1} in the activated state) (5). This method of study of the photochrome-impregnated polymers is out of the scope of the present work, but it may serve as a basis for future investigations.

The temperature-dependent rate constants obtained for the different photochromic species studied in this work may be used to calculate the energy of activation of the relaxation reaction. The energy of activation is a measure of the magnitude of the energy barrier which a reaction must overcome in order for it to proceed. The next section discusses the activation energies which were experimentally obtained for the relaxation reactions of plastic samples containing mercury bisdithizonate and phenyl mercury dithizonate.

Determination of the energy of activation of the relaxation reaction. In order to calculate the activation energy of the relaxation reaction, the time constants, representing

the time required for the excited state population to reach 1/e of its maximum value, were calculated from the rate constants. From Equation (11), the relaxation time constant, tau (τ), is simply the inverse of the relaxation rate constant, k. Table 4 lists the relaxation time constants, tau (τ), associated with each of the samples at different sample temperatures. Also from Equation (11), a linear relationship should exist between the logarithim of tau (τ) and the inverse sample temperature. This type of plot is an Arrhenius plot and is used to calculate the activation energy of a thermally-dependent reaction.

Table 4. Relaxation time constants (τ) for CAB-film samples of mercury bisdithizonate and phenyl mercury dithizonate (samples I through IV).

Temperature (K)	1/T (10^3 K^{-1})	τ_I	τ_{II}	τ_{III}	τ_{IV}
		(seconds)		(seconds)	
363	2.75	909	917	-	384
353	2.83	1218	1502	549	625
333	3.00	5814	7407	3356	4695
303	3.30	-	12500	11111	9346
283	3.53	>22371	30303	37453	47170

Figures 24 and 25 are semilogarithmic plots of 1/k, or τ (sec.), versus inverse sample temperature for the mercury bisdithizonate and phenyl mercury dithizonate samples under consideration. From the calculated slopes, the energy of activation of the sample containing mercury bisdithizonate is $E_a = 0.16 \pm .05$ eV. This value of the activation energy for mercury bisdithizonate is in fair agreement with that reported for the relaxation of 1% mercury bisdithizonate in polymers other than CAB. Activation energies of 0.178 - 0.716 eV have been reported for the relaxation reaction of the photochromic molecule in various polymers (19). The experimentally determined activation energy calculated for CAB samples containing phenyl mercury dithizonate is $E_a = 0.22 \pm .05$ eV. The activation energy for the single-ligand species is slightly larger than that of the dual-ligand species.

Aside from the relatively large experimental errors associated with the activation energies, the difference in the activation energies associated with the relaxation reactions of the excited phenyl mercury dithizonate and mercury bisdithizonate molecules may be interpreted in several ways. First, the higher activation energy for the phenyl mercury dithizonate species would indicate that a relatively large energy barrier must be surmounted in order for the relaxation of the excited state phenyl mercury dithizonate to proceed. This relatively large energy barrier may be the result of the single-ligand molecule becoming chemically attached to the polymer matrix. The attachment of the photochromic molecule to the polymeric chain would most likely cause an increase in the steric hindrance of the isomerization reaction. The added steric hindrance would result in a relatively large activation energy for the relaxation reaction of the polymer-phenyl mercury dithizonate complex.

The lower activation energy associated with the relaxation of the excited state mercury bisdithizonate species indicates that the isomerization from the excited state to the ground state occurs more readily in this case than in the single-ligand case. The easier relaxation transition of the two-ligand molecule may be the result of some

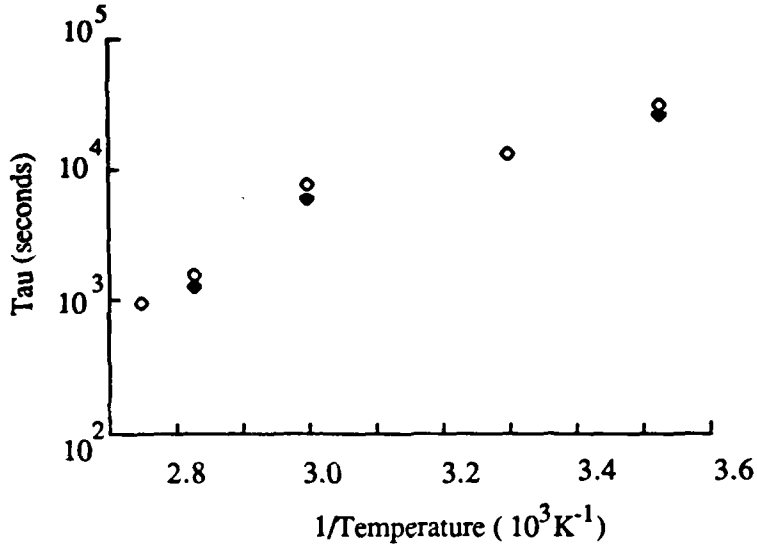

Figure 24. Semilogarithmic plot of tau (τ, sec.) versus inverse temperature for the relaxation of 0.2% (closed diamond) and 0.4% (open diamond) mercury bisdithizonate.

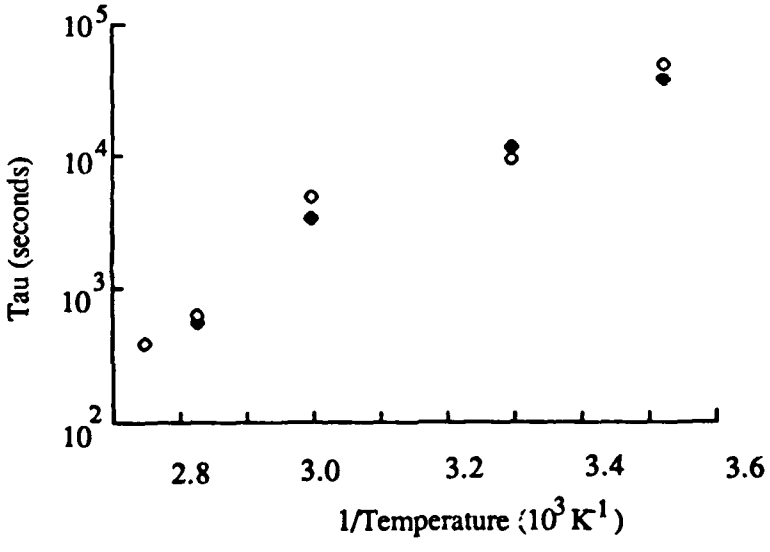

Figure 25. Semilogarithmic plot of tau (τ, sec.) versus inverse temperature for the relaxation of 0.26% (closed diamond) and 0.53% (open diamond) phenyl mercury dithizonate.

cooperative interaction between the two ligands of the mercury bisdithizonate photochromic molecule which results in a lower activation energy for the relaxation reaction. However, this cooperative effect of the two-ligand species is not consistent with the earlier statement made about the (presumed) non-interaction of the two ligands of the mercury bisdithizonae molecule when in solutions of chloroform or carbon tetrachloride (5). Thus, some other mechanism may be happening to lower the activation energy of the dual-ligand species.

This chapter has discussed the general considerations regarding the photo-isomerism of photochromic molecules in CAB polymer matrices. The relaxation reaction has been examined in detail and the reaction rate constants and activation energies have been presented. The steric effects of the polymer matrix associated with the physical rearrangement of the photochromic molecules have been discussed. The next chapter will examine the wavelength dependence of the excitation reaction of the photochrome-polymer systems. Chapter VII will also examine the dependence of the excitation reaction on the photochromic composition and concentration of the plastic samples.

Chapter VII - Dependence of the Excitation Reaction on Write Beam Wavelength and Photochromic Sample Composition

Dependence of the excitation reaction on incident write beam wavelength. It was shown in Chapter IV that the maxima of the ground state (visible) absorbance spectra of the mercury bisdithizonate and the phenyl mercury dithizonate samples occur at 485 nm. and 476 nm., respectively. To determine the relative sensitivity of the excitation reaction of both of these compounds to the two available write beam wavelengths, 488.0 nm. and 514.5 nm., plastic samples containing each of the photochromic species were exposed to an incident write beam intensity range of approximately 10 - 150 W/cm^2. Tables 5 through 8 list the times required to reach a particular HeNe probe beam transmission level under various conditions of sample temperature, incident light wavelength and intensity. The following section is a discussion of the experimentally observed dependence of the excitation of the photochromic samples on incident write beam wavelength.

The Reciprocity Law discussed in Equation (2) of Chapter II predicts that, for a given optical density, a log-log plot of the exposure intensity vs. the exposure time required to reach the desired optical density should be linear. Figures 26 and 27 are log-log plots of the write beam intensity (λ = 488.0 nm. and 514.5 nm.), vs. exposure time to reach a 50% HeNe transmission level (OD 0.3) for samples containing 0.4% mercury bisdithizonate and 0.53% phenyl mercury dithizonate, respectively. The sample temperature in each case was 50°C. The writing times using the 514.5 nm. wavelength writing beam (solid diamonds) were about 60% of those when using the 488.0 nm. wavelength writing beam (open diamonds). As predicted, each of the plots represent a reasonably straight line. The data in Tables 5 through 8 indicate the 514.5 nm. wavelength writing beam also wrote faster to other HeNe transmission levels than did

Table 5. Exposure time (in msec.) to reach 80%, 50%, and 30% HeNe transmission values for samples containing 0.2% mercury bisdithizonate (sample I) and 0.4% mercury bisdithizonate (sample II). Writing wavelength is 488.0 nm. Writing intensity range is 10 - 100 W/cm^2.

Sample			I			II	
Temp. (°C)	Intensity (W/cm^2)	80%	50%	30%	80%	50%	30%
90	100	.893	5.14	18.4	.575	2.71	6.97
	50	1.56	9.37	34.8	.937	5.21	14.0
	10	7.90	50.3	186	5.87	28.4	79.9
50	100	1.06	7.00	24.4	.740	4.32	11.4
	50	1.75	13.0	50.4	1.30	7.74	20.4
	10	8.32	66.6	271	7.33	45.7	131
10	100	1.53	9.53	29.6	1.00	4.99	12.2
	50	2.47	16.7	54.2	1.95	9.42	22.4
	10	12.1	82.0	281	8.65	51.6	140

Table 6. Exposure time (in msec.) to reach 80%, 50%, and 30% HeNe transmission values for samples containing 0.26% phenyl mercury dithizonate (sample III) and 0.53% phenyl mercury dithizonate (sample IV). Writing wavelength is 488.0 nm. Writing intensity range is 10 - 100 W/cm^2.

Sample			III			IV	
Temp. (°C)	Intensity (W/cm^2)	80%	50%	30%	80%	50%	30%
90	100	1.46	6.78	17.8	1.32	5.27	10.9
	50	2.27	10.9	28.7	2.11	9.64	20.8
	10	12.7	60.5	161	10.8	54.4	119
50	100	1.37	7.30	20.2	1.36	6.15	13.0
	50	2.48	12.6	35.0	2.93	13.4	28.8
	10	10.5	59.1	176	10.7	56.0	129
10	100	2.17	10.6	24.8	1.91	8.93	17.4
	50	3.82	18.6	43.3	4.23	16.4	32.4
	10	19.1	96.7	244	23.5	90.4	188

Table 7. Exposure time (in msec.) to reach 80%, 50%, and 30% HeNe transmission values for samples containing 0.2% mercury bisdithizonate (sample I) and 0.4% mercury bisdithizonate (sample II). Writing wavelength is 514.5 nm. Writing intensity range is 10 - 150 W/cm^2.

Sample		I			II		
Temp. (°C)	Intensity (W/cm^2)	80%	50%	30%	80%	50%	30%
90	150	.450	2.48	13.2	.344	1.03	3.85
	100	.550	3.43	16.2	.458	2.00	5.71
	50	.940	6.47	31.9	.825	4.18	11.7
	10	3.96	28.6	123	2.73	20.6	62.4
50	150	.550	3.52	15.8	.473	2.08	5.39
	100	.691	4.62	19.8	.550	2.65	6.96
	50	1.05	7.11	28.1	.940	5.13	13.0
	10	4.56	30.3	119	4.58	24.6	64.6
10	150	.595	4.00	16.3	.568	2.75	6.52
	100	.960	6.43	22.7	.783	3.82	8.67
	50	1.64	11.4	40.1	1.40	7.01	17.0
	10	6.60	50.3	205	6.22	34.3	88.9
-20					.897	4.38	9.87
					.970	5.30	12.7
					1.51	7.96	20.0
					6.05	32.3	83.0

Table 8. Exposure time (in msec.) to reach 80%, 50%, and 30% HeNe transmission values for samples containing 0.26% phenyl mercury dithizonate (sample III) and 0.53% phenyl mercury dithizonate (sample IV). Writing wavelength is 514.5 nm. Writing intensity range is 10 - 150 W/cm^2.

Sample			III			IV	
Temp. (°C)	Intensity (W/cm^2)	80%	50%	30%	80%	50%	30%
90	150	.660	3.83	11.4	.640	2.62	5.80
	100	.772	5.31	16.7	.788	3.41	7.70
	50	1.52	9.55	32.0	1.27	6.21	14.5
	10	5.43	35.9	120	2.02	29.9	71.6
50	150	.895	5.93	18.1	.600	2.93	6.48
	100	1.23	7.73	23.4	.857	3.98	8.91
	50	2.43	14.3	39.2	1.68	7.24	16.1
	10	10.5	62.8	180	7.21	34.9	79.1
10	150	1.06	6.84	19.2	.883	4.91	10.4
	100	1.38	9.30	24.8	1.06	6.04	12.6
	50	2.82	18.0	49.2	1.92	9.84	21.9
	10	14.2	91.6	282	7.38	40.4	98.6

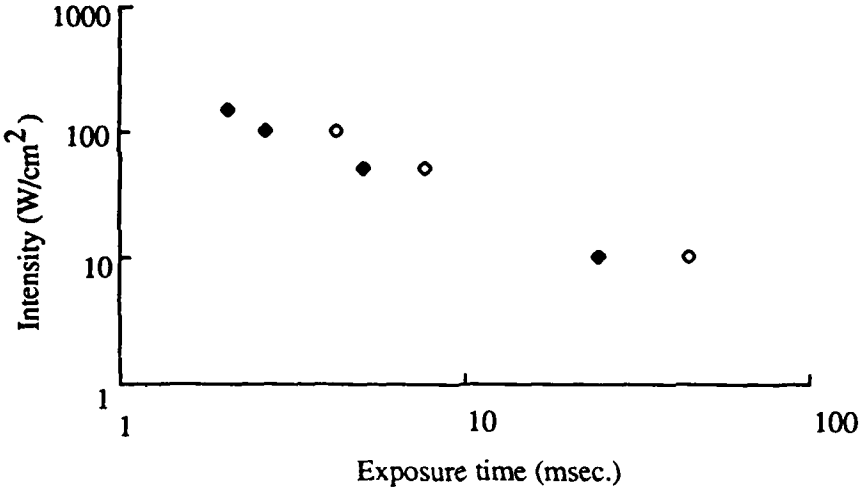

Figure 26. Write beam intensity (W/cm^2) vs. exposure time (msec) to reach 50% transmission for 0.4% mercury bisdithizonate sample. Write beam wavelength: closed diamond, 514.5 nm.; open diamond, 488.0 nm. Sample temperature, 50°C.

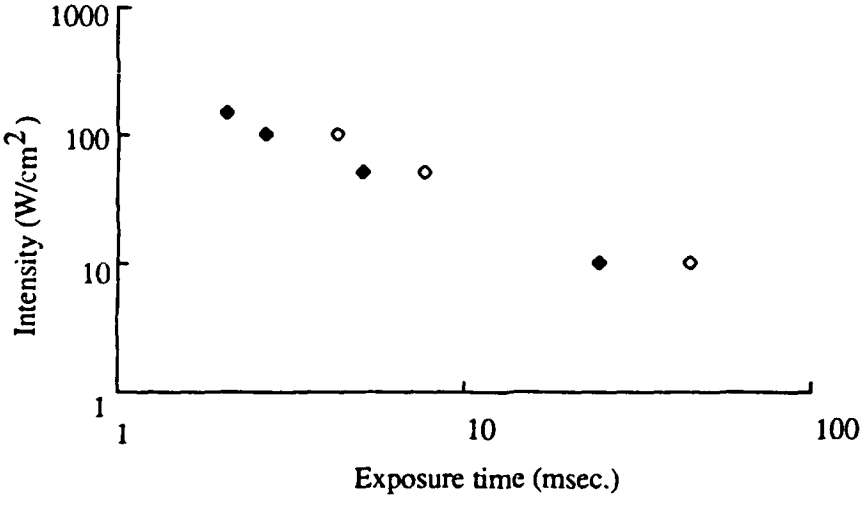

Figure 27. Write beam intensity (W/cm^2) vs. exposure time (msec) to reach 50% transmission for 0.53% phenyl mercury dithizonate sample. Write beam wavelength: closed diamond, 514.5 nm.; open diamond, 488.0 nm. Sample temperature, 50°C.

the 488.0 nm. wavelength write beam for both of the photochromic species at sample temperatures of 10°C and 90°C.

The increased sensitivity of the photochromic samples to the 514.5 nm. wavelength over that of the 488.0 nm. wavelength was unexpected. From Chapter IV, the major absorption peaks of both phenyl mercury dithizonate and mercury bisdithizonate are around 475 - 485 nm., and one would have expected the 488.0 nm. wavelength write beam to write faster than the 514.5 nm. wavelength write beam. The higher optical density at 488.0 nm. indicates that more optical energy is being absorbed by the molecules at this wavelength than at 514.5 nm. Due to the large absorption of the mercury bisdithizonate sample at 514.5 nm., it is not surprising to observe relatively short writing times at this longer wavelength. However, since more optical energy at the lower wavelength is absorbed by the ground state molecules, one would expect that the excitation reaction would occur more quickly and lead to shorter writing times when using the lower wavelength writing beam. We do not understand this result.

Dependence of the photochromic excitation reaction on photochrome concentration and species. In order to observe the effect on the writing times of the photochromic samples when the photochrome concentration was varied, samples containing different concentrations of photochromic species were exposed to write beam intensities of 10 - 150 W/cm^2 at a wavelength of 514.5 nm. and at sample temperatures ranging from 10 - 90°C. The following is a discussion of the major trends which were observed in the data.

Figures 28 and 29 are log-log plots of the write beam intensity (λ = 514.5 nm.) vs. time (msec.) to write to a 50% HeNe level transmission for samples containing mercury bisdithizonate (0.2% and 0.4%) and phenyl mercury dithizonate (0.26% and 0.53%), respectively. The sample temperature in all cases is 50°C. The samples containing the higher concentration of either photochromic species wrote faster than the sample containing the lower concentration of the same species. From Tables 5 through

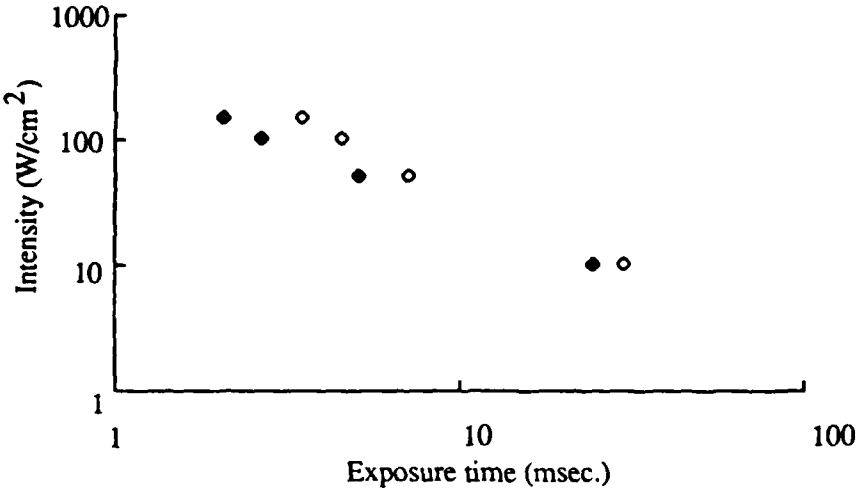

Figure 28. Write beam intensity (W/cm^2) vs. exposure time (msec) to reach 50% HeNe transmission for samples containing 0.2% (open diamond) and 0.4% mercury bisdithizonate (closed diamond) (samples I and II). Write beam wavelength is 514.5 nm. Sample temperature, 50°C.

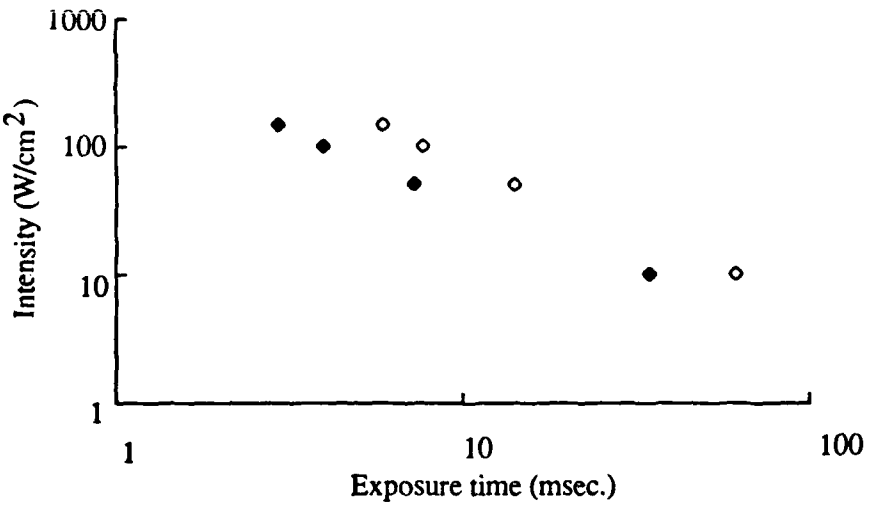

Figure 29. Write beam intensity (W/cm^2) vs. exposure time (msec) to reach 50% transmission for samples containing 0.26% (open diamond) and 0.53% phenyl mercury dithizonate (closed diamond) (samples III and IV). Write beam wavelength is 514.5 nm. Sample temperature, 50°C.

8, the same concentration dependent increase in the writing speed is observed at sample temperatures of 90°C and 10°C.

The data in Tables 5 through 8 also show another important feature of the behavior fo the photochromic samples. The much shorter writing time to the 30% HeNe transmission level observed in the higher concentration samples of both photochromic species further illustrates the concentration dependence of the absorbance of the photochromic molecules. The higher concentration of molecules does not increase the rate at which the individual molecules isomerize (assuming no interaction between photochromic molecules is present), but it does lead to higher optical densities in a shorter time than does a less concentrated sample. The decrease in the time required to reach a relatively high optical density upon exposure of a highly concentrated sample is due to the presence of a larger number of absorbing molecules. Even though the rate of conversion from the ground state to the excited state may be the same in different samples containing different concentrations of the same photochromic species, the fact that one sample contains more of the absorbing species than the other allows a particular optical density to be reached in a shorter time than in the lower concentration sample.

The speed of the excitation reaction is also dependent on the type of photochromic species present in the sample. Figure 30 shows log-log plots of the intensity (λ = 514.5 nm.) vs. exposure time to reach a HeNe read beam transmission of 50% for samples containing 0.4% mercury bisdithizonate (closed diamond) and 0.53% phenyl mercury dithizonate (open diamond). The sample temperature in each case was 50°C. The two-ligand mercury bisdithizonate species wrote faster than the single-ligand phenyl mercury dithizonate over the entire 10 - 150 W/cm^2 write beam intensity range. The faster writing speed of the mercury bisdithizonate over that of the phenyl mercury dithizonate is due to the fact that even though each sample has the same number of molecules, the dual-ligand species has twice as many photo-reactive sites than does the single ligand species. Each of the dithizonate ligands is an independent center of photochromic activity. Thus, the

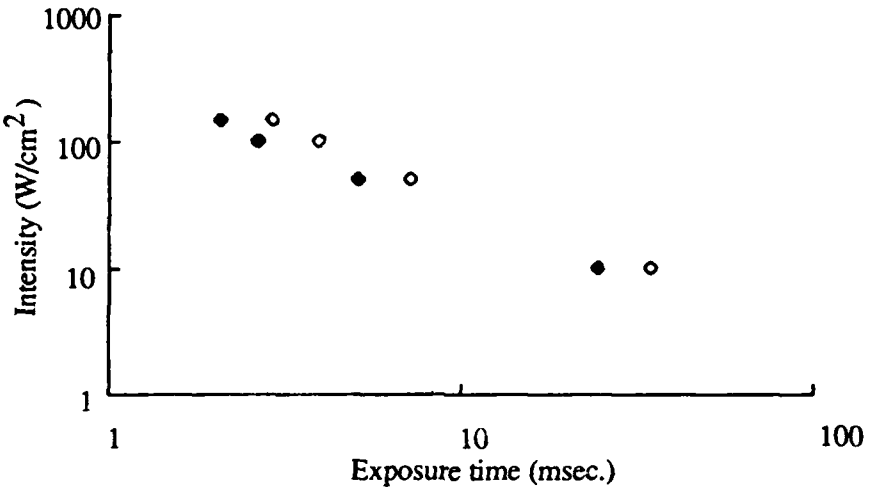

Figure 30. Write beam intensity (W/cm^2) vs. exposure time (msec) to reach 50% transmission for samples containing 0.4% mercury bisdithizonate (closed diamond) and 0.53% phenyl mercury dithizonate (open diamond) (samples II and IV). Write beam wavelength is 514.5 nm. Sample temperature, 50°C.dual-ligand mercury bisdithizonate species writes faster than the single-ligand phenyl mercury dithizonate species.

Since these results indicate that the mercury bisdithizonate species writes faster than the phenyl mercury dithizonate species, we will concentrate on the dual ligand species in further writing experiments. In addition, since faster writing times are obtained with the green 514.5 nm writing wavelength, this will be used exclusively. The next chapter will use the results presented in this chapter to further investigate the high speed writing possibilities of the photochromic mercury bisdithizonate samples.

Chapter VIII - High Speed Writing Using Mercury Bisdithizonate

High speed writing experiments

The previous results indicated that the samples containing mercury bisdithizonate wrote faster than those containing phenyl mercury dithizonate. In order to see how fast one could write onto the samples, writing experiments using high laser intensities were performed on samples containing 0.2%, 0.5%, and 1.0% mercury bisdithizonate (samples V-2, V-3, and V-4). Since previous results also indicated that the photochromic samples wrote faster using the 514.5 nm. write beam wavelength instead of the 488.0 nm. write beam wavelength, all of the high speed writing experiments were performed using a write beam intensity range of 10 - 800 W/cm^2 at a wavelength of 514.5 nm.

The exposure times required to reach specific HeNe transmission values for the mercury bisdithizonate samples at temperatures of 10°C, 50°C, and 90°C are listed in Table 9. The writing times listed for the intensities marked with an asterisk, (*), were obtained using the high intensity experimental setup (200 - 800 W/cm^2) as described in Chapter III. The rest of the data was obtained using the medium intensity experimental setup (10 - 150 W/cm^2) as described in Chapter III.

The writing times listed in Table 9 for sample V-2 using the 10 - 150 W/cm^2 writing intensity range are in good experimental agreement with the previously reported writing times corresponding to sample I under the same conditions of write beam intensity and temperature (Table 7). Both of the samples, V-2 and I, contain 0.2% mercury bisdithizonate. However, the samples were made over two years apart (sample I, 10/84; sample V-2, 1/87), and it was important to make sure that both samples behaved in a similar manner under the same writing conditions. Both of the samples

Table 9. Exposure time (in msec.) to reach 80%, 50%, and 30% HeNe transmission values for samples containing 0.2% (sample V-2), 0.5% (sample V-3), and 1.0% (sample V-5) mercury bisdithizonate. Writing wavelength is 514.5 nm. Writing intensity range is 10 - 800 W/cm^2. Intensities marked with an asterisk (*) represent the highest intensity setup.

Sample		V-2 (0.2%)			V-3 (0.5%)			V-4 (1.0%)		
Temp. (°C)	Intensity (W/cm^2)	80%	50%	30%	80%	50%	30%	80%	50%	30%
90	800*	.081	.433	1.16	.071	.341	.961	.071	.317	.751
	400*	.139	.813	2.54	.144	.794	1.90	.138	.610	1.50
	200*	.274	1.58	4.44	.283	1.73	4.79	.240	1.17	2.99
	150	.493	2.22	7.41	.485	2.22	5.73	.590	2.32	5.27
	100	.690	3.84	12.9	.630	2.94	7.77	.703	3.08	7.15
	50	.980	5.76	21.7	1.02	5.30	14.1	.983	4.70	11.8
	10	5.90	32.9	108	5.85	33.1	87.4	7.03	32.4	91.9
50	800*	.090	.581	1.73	.084	.422	1.08	.086	.383	.839
	400*	.201	1.16	3.28	.162	.818	2.13	.161	.781	1.78
	200*	.378	2.02	4.94	.290	1.65	4.41	.270	1.46	3.49
	150	.745	3.78	11.0	.524	2.49	6.56	.609	2.53	5.54
	100	.803	4.75	13.8	.733	3.84	9.65	.726	3.18	7.36
	50	1.44	9.44	29.1	1.11	6.04	15.0	1.31	6.18	14.3
	10	6.66	38.6	124	5.70	33.6	92.2	6.07	33.0	86.4
10	800*	.136	.858	2.35	.092	.455	1.15	.097	.445	.977
	400*	.258	1.36	3.83	.208	1.11	2.75	.228	1.08	2.20
	200*	.485	2.27	5.31	.348	1.86	4.94	.338	1.82	4.02
	150	.560	3.36	10.8	.690	3.39	8.04	.768	2.93	6.12
	100	.973	5.39	17.0	1.06	5.26	12.7	.885	3.76	8.04
	50	1.98	10.2	31.2	1.79	9.03	21.6	1.55	7.47	16.5
	10	10.2	60.3	198	10.8	60.3	157	7.30	40.0	100

were characterized on similar experimental setups, although some improvements in the alignment of the write and read beams were used when characterizing the V-2 sample. One source of the slight discrepancies between the data obtained from the two different samples may be due to an aging process associated with the polymer-photochrome system. Photolysis of the polymer (20) or oxidation of the photochromic molecules (3) may occur which would alter the results of the writing experiments. More importantly however, are the experimental errors associated with the setups. The error involved in the observed writing times using a particular experimental setup may be as large as 15 - 20 percent between data runs.

From the data listed in Table 9, a decrease in the writing time to a particular HeNe read beam transmission with increased sample concentration or temperature is still evident. As the photochrome concentration increases from 0.2% to 0.5%, the exposure time required to write to any particular HeNe read beam transmission is decreased. The V-3 sample, with 0.5% mercury bisdithizonate, wrote faster in most cases than did sample V-2, which contained 0.2% mercury bisdithizonate. This concentration-dependent effect is not as pronounced here as when comparing the writing times associated with samples I and II, or samples III and IV (Tables 7 and 8). Comparison of the writing times for sample V-4 (1.0% mercury bisdithizonate) with those for V-3 indicates that only a small increase in the writing speed is obtained when one increases the concentration of mercury bisdithizonate from 0.5% to 1.0%. For each of the experimental writing intensities, the time required to write to a particular HeNe transmission is similar in both the 0.5% and 1.0% mercury bisdithizonate samples. The less concentrated sample is nearly as fast as the more concentrated sample. This effect suggests that an upper limit in the writing speed is approached in a mercury bisdithizonate concentration range of 0.5 - 1.0%. The higher concentration coincides with the maximum amount of mercury bisdithizonate which can be put into the CAB plastic. Due to the relatively low solubility of mercury bisdithizonate in CAB plastic,

precipitation of the photochrome from the polymer occurs at a concentration of about 1% (20).

Throughout the writing experiments, the experimentally observed writing time to reach a particular HeNe transmission decreases as the write beam intensity increases. This trend toward faster writing times was observed over the entire 10 - 800 W/cm^2 write beam intensity range. Generally, the increase in the incident intensity with a decrease in the writing time to a particular HeNe transmission value should follow the Reciprocity Law for photosensitive materials as discussed in Chapter II (Equation 2) and the results section of Chapter VII. In this section, the writing beam intensity range is larger than was previously discussed. Thus, a better understanding of the relationship of the Reciprocity Law and the photochromic mercury bisdithizonate species may be found here. The following section is a discussion of the application of the Reciprocity Law to some of the photochromic samples used in this study.

Verification of the Reciprocity Law

Figures 26 and 27 are log-log plots of the write beam intensity (W/cm^2) versus exposure time (msec.) to reach 50% HeNe transmission (OD = 0.3) for samples containing 0.2% and 0.5% mercury bisdithizonate, respectively. The closed symbols represent the data obtained using the 10 - 150 W/cm^2 intensity experimental setup and the open symbols correspond to the data obtained using the 200 - 800 W/cm^2 intensity experimental setup. The results support the idea that the exposure time required to reach a particular optical density decreases linearly as the write beam intensity increases. The linearity of the plots over the full range of intensities also provides some qualitative measure of the experimental precision of the writing times obtained from both the medium and high intensity experimental setups. The maximum available intensity using the medium intensity setup was 150 W/cm^2, wheras the minimum intensity of the high intensity setup was 200 W/cm^2. Although no explicit overlap in the available intensities is present, extrapolation of the data obtained from either experimental setup indicates that

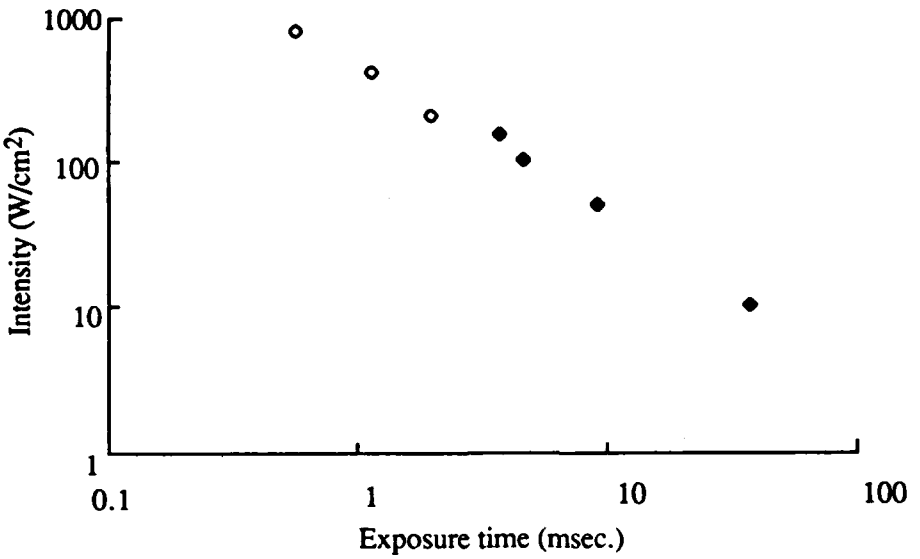

Figure 26. Write beam intensity (W/cm^2) versus exposure time (msec.) to reach 50% HeNe transmission for 0.2% mercury bisdithizonate (sample V-2) at a sample temperature of 50°C. Closed diamond, medium intensity experimental setup; Open diamond, high intensity experimental setup. Write beam wavelength, 514.5 nm.

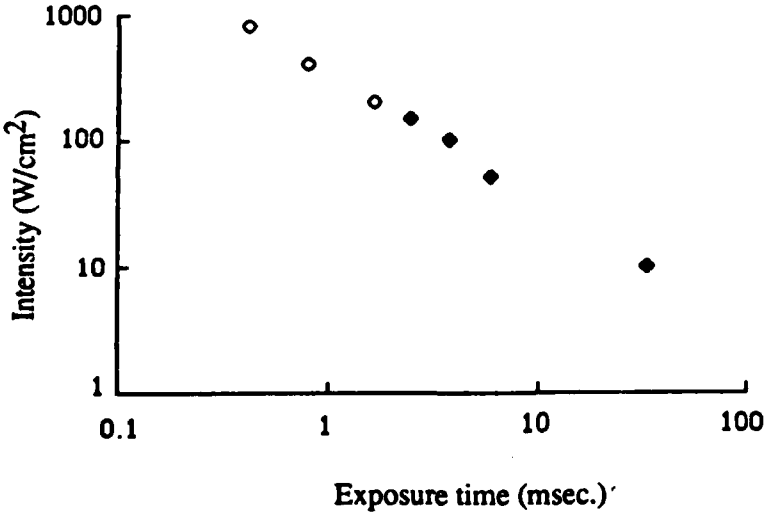

Figure 27. Write beam intensity (W/cm^2) versus exposure time (msec.) to reach 50% HeNe transmission for a sample containing 0.2% mercury bisdithizonate (sample V-2) at a sample temperature of 50°C. Closed diamond, medium intensity experimental setup; Open diamond, high intensity experimental setup. Write beam wavelength, 514.5 nm.

the two sets of data are consistent. This characteristic is important if one is to compare the data from two different experimental setups. From Figure 26, the slope of the plot of the data (at 50°C) for the 0.2% mercury bisdithizonate is 1.03 ± 0.1, which is in very good agreement with the reciprocity law (Equation (2)) of Chapter II. Thus, the reciprocity law appears to hold quite well at 50°C over the ranges of exposure intensities and exposure times required to reach a 50% HeNe transmission level. A comparison of similar plots for a mercury bisdithizonate sample at temperatures of 10°C and 90°C further supports the Reciprocity Law relationship of the photochromic material.

Figure 27 shows log-log plots of the intensity (W/cm^2) versus time (msec.) to reach 50% HeNe transmission for a sample containing 0.5% mercury bisdithizonate (sample V-3) at sample temperatures of both 10°C and 90°C. The intensity range is 10 - 800 W/cm^2 at a wavelength of 514.5 nm. The higher sample temperature leads to decreased writing times at all write beam intensities. Each plot shows good linearity, with slopes of 0.87 ± 0.1 and 0.95 ± 0.1 for the 10°C and 90°C data, respectively. The slope obtained from the higher sample temperature data is in good agreement with the predicted slope of unity from the reciprocity law. The lower sample temperature resulted in a plot with a slope having a greater deviation from unity.

Overall, the writing times using the low-temperature, low-intensity setup are clearly longer than those obtained using the higher-temperature, higher-intensity setup. However, the Reciprocity Law appears to hold reasonably well over the write beam intensity range used for the entire sample temperature range of 10 - 90°C.

Another trend which is apparent is the temperature dependence of the excitation reaction generally decreases as the incident writing intensity increases . The writing times to a particular HeNe read beam transmission are less affected by a change in the sample temperature when the higher write beam intensities are used to excite the photochromic molecules. Conversely, the writing speeds associated with the lower write beam intensities appear to be more dependent on the sample temperature. This idea will

be developed further in the next section concerning local heating and sample damage of the polymer by high intensity illumination.

Local sample heating and sample damage

One explanation for the decrease in the temperature dependence of the excitation reaction as the incident intensity increases is due to an increase of the local sample temperature as the incident intensity increases. The local heating of the plastic due to the incident beam may raise the local temperature sufficiently to allow for easier isomerism of the ground state molecules. Thus, at moderate temperatures, the local sample temperature may be effectively raised by a high incident intensity to causing an increase in the isomerization of the photochromic molecules similar to that which occurs at higher temperatures. However, at the lower write beam intensities, the incident energy input will not produce a sufficient local temperature change in the sample.

The energy input to the local area can be calculated from the incident intensity and the area of the affected region. For a 1 msec. duration of an incident intensity of 400 W/cm^2 over an area of approximately 0.01 cm. in diameter, the energy input is about 32 μJ. The specific heat of the CAB plastic is 0.3 - 0.4 cal/g°C (approx. 1.46 J/g°C) and the density of the CAB polymer is 1.25 g/cm^3 (see Table 2). If all of the energy goes into heating a volume of 10^{-6} cm^3 (corresponding to a depth of 0.01 cm.), the temperature increase is about 18°C. Assuming that the thermal conductivity of the plastic is so poor that no heat flows away from the target area during the short exposure time, then a 3 msec. shot at 400 W/cm^2 would lead to a temperature increase of about 54°C. This change in local sample temperature may lead to an effective target area temperature of 144°C if the sample temperature is 90°C. CAB notably softens at temperatures above 135°C. If the input energy cannot be dissipated fast enough, then thermal agitation will destroy the bonds within the polymer chains and physical damage to the sample will result. Furthermore, if the front layer of the absorbing medium

effectively absorbs all of the optical energy, then the effective thickness of the sample decreases and the resulting temperature change is greatly increased.

During some of the high speed writing experiments, the samples containing photochromic molecules did become visibly damaged when exposed to write beam intensities of 400 and 800 W/cm^2. A sample of the CAB plastic containing no photochromic molecules showed no damage when exposed to an incident write beam intensity of 800 W/cm^2 for more than 6 seconds. Presumably, the photochromic molecules absorb the incident energy and become thermally agitated. These agitated molecules transfer the heat to the surrounding plastic polymer chains. Since the polymer chains are relatively poor thermal conductors, they are unable to dissipate the heat efficiently. Consequently, polymer bonds are broken and visible cratering of the plastic surface occurs.

In order to gain a semi-quantitative estimate on the incident optical energy required to cause appreciable damage (energy damage threshold), microscopic investigations were performed on a photochromic sample which had been subjected to various exposures to a high intensity write beam . Experiments in which a 0.53% phenyl mercury dithizonate sample was exposed to an incident argon beam intensity of 500 W/cm^2 (λ = 488.0 nm.) for 2, 3, 4, 5, 6, and 7 milliseconds showed increasing amounts of damage as the exposure time increased beyond 3 msec. The beam diameter was approximately 0.300 mm. The sample temperature was 50^{o}C. The 3 - 7 millisecond exposures resulted in pitting, or cratering, of the sample. An increase in the exposure time led to an increase in the size of the pit. The 2 msec. exposure corresponds to a local temperature rise of roughly 44^{o}C. One estimate of the damage threshold energy may therefore be roughly 1 J/cm^2. A closer examination of the damaged area provides further insight into the ablation process.

Measurements of the crater size caused by the 6 msec. exposure under the conditions noted previously showed a diameter of approximately 60 μm. The

observation that the apparent diameter of the damaged spot is considerably less than the beam diameter indicates that the intensity on the central axis of the beam is greater than the intensity away from the central axis. The relatively large central peak intensity is indicative of the Gaussian profile of the laser beam. For a measured sample plane intensity of 500 W/cm^2, the central intensity peak may be as high as 850 W/cm^2 (corresponding to an aperture radius r = 50 μm., and a beam radius a = 75 μm.). The 6 msec. exposure would lead to a temperature rise at the very center of the sample target of about 230°C. This large temperature change would certainly raise the local temperature high enough to cause considerable damge.

In an attempt to reduce the sample damage effects caused by local heating, the sample temperature was reduced. Presumably this would require substantialy more heating before the sample melting point would be reached. Accordingly, writing experiments using high write beam intensities at a sample temperature of -30°C were performed. Table 10 lists the writing times to 80%, 50%, and 30% HeNe transmission values for samples V-2 and V-4 when exposed to write beam intensities of 200, 400, and 800 W/cm^2 at -30°C. The exposure times required to reach a particular HeNe transmission at a sample temperature of -30°C are greater than those required for the higher sample temperatures. However, the writing times to 50% HeNe transmission using the higher intensities are still under one millisecond.

Sample damage was still observed in those samples exposed to the 400 and 800 W/cm^2 intensities. No sample damage was observed in those samples exposed to the 200 W/cm^2 intensity. The presence of the damage at -30°C despite a relatively small estimate for the local target temperature of around 0°C, supports the claim that the primary damage is caused by the large central intensity of the incident Gaussian writing beam or that the light is being absorbed by the front portion of the sample thickness.

Table 10. Exposure time (in msec.) to reach 80%, 50%, and 30% HeNe transmission values for 0.2% and 1.0% mercury bisdithizonate samples (V-2, V-4). Writing wavelength is 514.5 nm. Writing intensity range is 200 - 800 W/cm^2.

Sample		V-2 (0.2%)			V-4 (1.0%)		
Temp. (°C)	Intensity (W/cm^2)	80%	50%	30%	80%	50%	30%
-30	800	.182	.830	2.52	.128	.470	1.11
	400	.270	1.40	4.21	.183	.711	1.69
	200	.582	3.48	9.18	.278	1.34	3.08

This chapter has presented the major experimental observations concerning the activation, or writing reaction of the CAB samples containing mercury bisdithizonate. The writing times to particular HeNe transmission levels using a wide range of incident write intensities have been presented and the coupled temperature-intensity dependence of the reaction has been discussed. Sample damage due to the local heating effects associated with a high intensity input have been presented and discussed. In the following chapter, all of the general conclusions which have been presented in this chapter and previous ones will be briefly reviewed.

Chapter IX - Conclusions

The experiments performed in the course of this work were designed to measure the optically induced excitation and thermal relaxation times of CAB polymer samples containing photochromic mercury bisdithizonate and phenyl mercury dithizonate molecules. Many experimental parameters were varied and different techniques were used to examine the photochromism associated with these molecular species. This chapter will briefly summarize the experimental results and conclusions which were found regarding the dependence of the excitation and relaxation reactions on photochromic species and concentration, excitation light intensity and wavelength, and sample temperature.

Generally, the speed of both the excitation and relaxation reactions of both species of photochromic molecules increased as the sample temperature increased. The reason for this temperature dependence is based on two concepts. An increase in the sample temperature increases the kinetic energy of the photochromic molecules and thereby allows for an easier physical isomerization of the molecules. An increase in the sample temperature will also increase the average microscopic polymer sample volume and allow for an easier isomerization of the molecules.

Samples containing the excited single-ligand phenyl mercury dithizonate species showed a faster relaxation from the excited state to the ground state than did samples containing the dual-ligand mercury bisdithizonate species. The excited state phenyl mercury dithizonate molecule is presumably able to thermally isomerize within the polymer substrate much easier than the excited state mercury bisdithizonate molecule since the single-ligand molecule is smaller than the dual-ligand molecule.

In addition, preliminary measurements indicate that the relaxation process is enhanced through absorption of the red reading beam. Although the intensity of this beam was kept low to minimize these effects, it may offer a means for achieving faster relaxation times.

Several features of the excitation reaction were studied. First, all of the samples unexpectedly showed a higher excitaion sensitivity to the 514.5 nm. wavelength write beam even though the ground state molecules of both the mercury bisdithizonate and phenyl mercury dithizonate species used in this work were more highly absorbing at 488.0 nm. The reason for this is not known.

Samples containing the dual-ligand mercury bisdithizonate species showed a faster excitation, or writing speed than did samples containing the single-ligand phenyl mercury dithizonate. Increasing the sample concentration of either photochromic species also increased the excitation speed of the sample. These trends were observed for all experimental temperatures and incident write beam intensities.

The speed of the excitation reaction increased as the incident excitation write beam intensity increased. This was evident at both the 488.0 nm. and 514.5 nm. wavelengths of the write beam.

Many of the experiments studying the faster writing times were confined to the mercury bisdithizonate samples and to the 514.5 nm writing wavelength because of these observed trends. Excitation, or writing speeds (to 50% read beam transmission) under 1 msec. were obtained for incident intensities of 400 and 800 W/cm^2 at a wavelength of 514.5 nm. The Reciprocity Law appeared to hold reasonably well over an incident intensity range of 10 - 800 W/cm^2. However, sample damage occurred due to local target heating if the incident intensity was too high. Lowering the sample temperature to -30°C reduced the excitation time slightly, but sample damage was still evident. An estimate of the sample damage threshold of the CAB-photochrome samples is 1 J/cm^2. However, limiting speeds were approached for mercury bisdithizonate

concentrations of 0.5 - 1%. These limiting speeds were the result of the first fractional part of the plastic sample absorbing most of the incident energy and effectively shadowing the remainder of the sample.

Our experiments indicate that this material may not be suited for the optical signal processing applications under consideration. Sample damage effectively limits both the absolute optical densities and the fastest writing times which can be reached. Attempts to limit this sample damage were unsuccessful. It appears that, as the sample is illuminated, the front layer of the sample absorbs sufficient energy to cause it to melt. The back portions of the sample are effectively shielded and the effective optical density of the sample is limited.

However, there are two positive observations which can be made. First, the material may have optical signal processing applications in a reverse mode. Since high optical densities naturally appear for the ground state absorption wavelengths, the writing wavelength would be used in the rf signal processor rather than the reading wavelength. If a desired rf frequency is to be passed, then the desired location on the photochromic should be strongly illuminated with the writing wavelength. That particular region would become more transparent to the writing wavelength. While unorthodox, this may allow the material to be used.

More importantly, the sample appears to be well suited for applications where moderately low optical densities of 0.3 are required at high speeds such as in optical data storage. In these applications, large optical densities are not required and this material displays impressive writing speeds of under 1 msec. We feel that this situation offers the greatest potential for this material and suggest that it be considered for these kinds of high speed, low optical density applications.

References

(1) G. H. Brown, Techniques of Chemistry: Photochromism (John Wiley and Sons, New York, 1972) Vol. III

(2) P. H. Vandewijer, G. Smets, J. Polymer Science: Part C 22, 231 (1968)

(3) E. B. Sandell, H. Onishi, Photometric Determination of Traces of Metals, Part 1 (J. Wiley and Sons, New York 1978) p. 581

(4) U. W. Grummt, H. Langbein, R. Noske, G. Robissch, J. Photochemistry 27, 249 (1984)

(5) L. S. Meriwether, E. C. Breitner, N. B. Colthup, J. Amer. Chem. Soc. 87: 20, 4448 (1965)

(6) T. Halloway, Senior Research Project, Physics Dept., San Diego State Univ.

(7) M. Thomas, Thesis, Physics Department, San Diego State University (1985)

(8) Kodak Plates and Films for Science and Industry, 1st ed., Eastman Kodak Co., Rochester, New York 1967

(9) D. Skoog, D. West, Analytical Chemistry, An Introduction (Holt, Rinehart, and Winston, Inc., New York, 1974) 2nd. Ed.

(10) A. Streitwieser, Jr., C. H. Heathcock, Introduction to Organic Chemistry (Macmillan Publishing Co., Inc., New York 1976) p. 46

(11) J. A. Brydson, Plastics Materials (Van Nostrand Reinhold Company, New York, New York. 1970) 2nd Ed.

(12) Handbook of Chemistry and Physics (Chemical Rubber Company, Cleveland, Ohio, 1971) 52nd. Ed.

(13) Catalog Handbook of Fine Chemicals (Aldrich Chemical Co. Milwaukee, Wisconsin 1974) p. 231

(14) R. D. Deanin, Polymer Structure, Properties and Applications (Cahners Publishing Company, Inc., Boston, Mass. 1972)

(15) A. Hutton, H. M. N. H. Irving, J. Chem. Soc. Dalton Trans. 1982

(16) E. B. Sandell, H. Onishi, Photometric Determination of Traces of Metals, Part 1 (J. Wiley and Sons, New York 1978) pp. 579-647

(17) M. Kryszewski, D. Lapienis, B. Nadolski, J. Polymer Science: Polymer Chem. Ed. 11, 2423 (1973)

(18) H. Kamogawa, J. Polymer Science: Part A-1 9, 335 (1971)

(19) M. Kryszewski, B. Nadolski, A. Fabrycy, Ann. Soc. Chim. Polonorum 49, 2077 (1975)

(20) L. Van Vlack, Elements of Materials Science and Engineering (Addison-Wesley Publishing Company, Reading Mass., 1980) 4th Ed. Chapter 7 p. 271

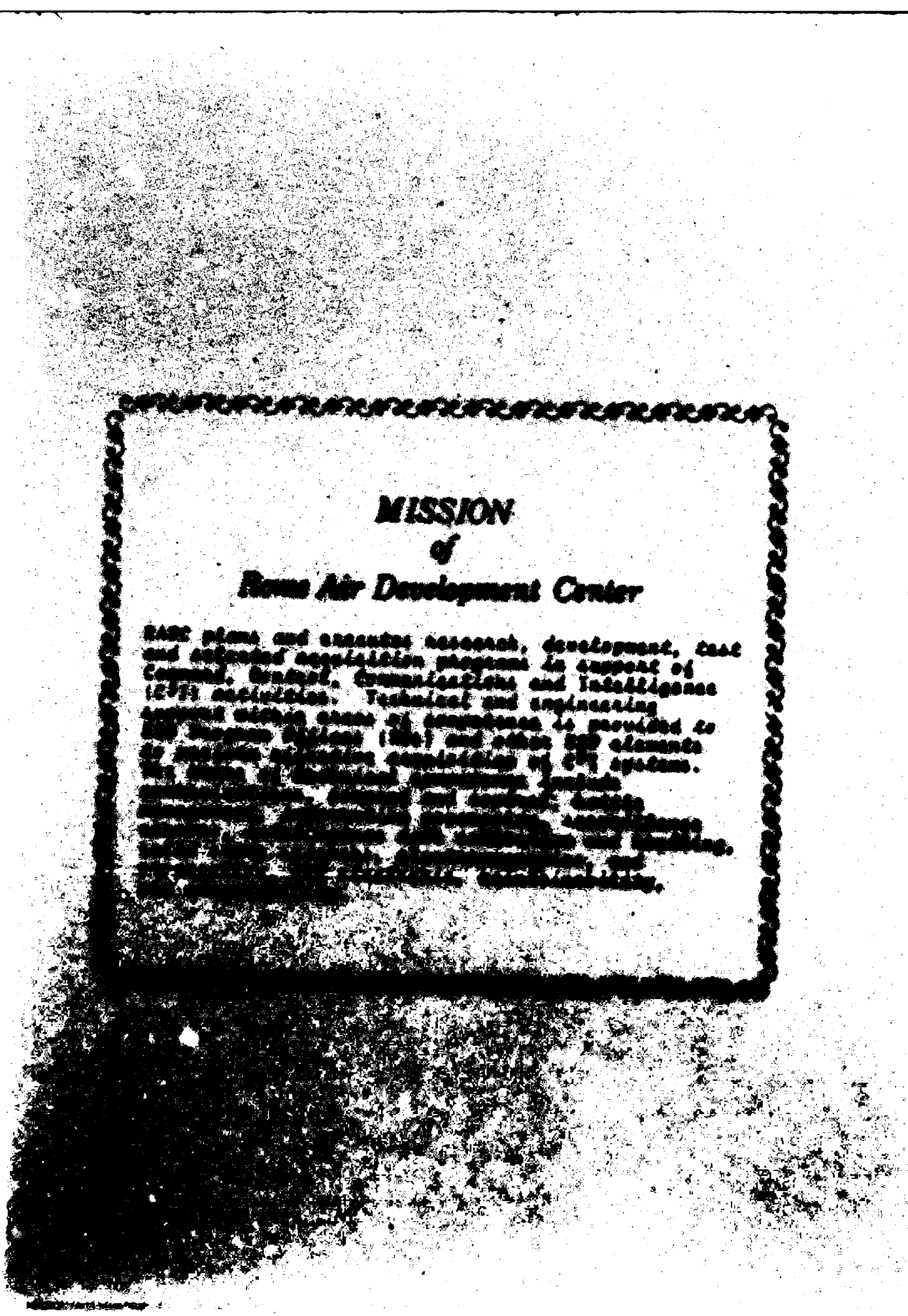
MISSION
of
Rome Air Development Center

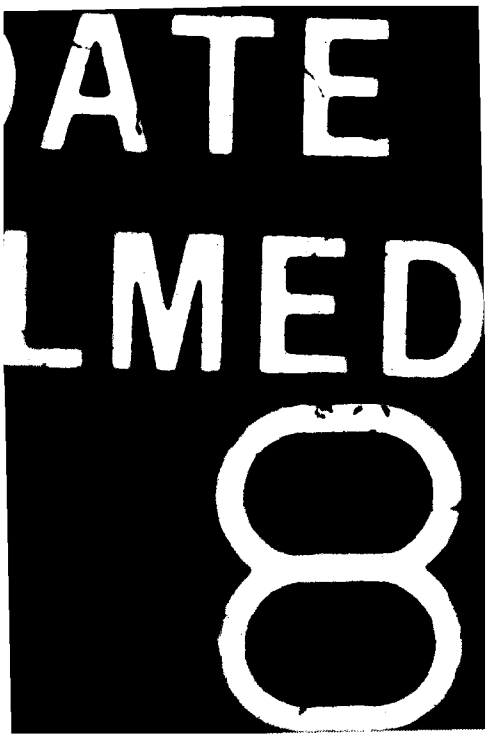
ATE
LMED
8